



Special Review

Review

Affordable High-performance Ti/TiB Metal Matrix Composites Tailored for Automobile Engine Components: Materials Design, Manufacturing Process, and Remaining Issues

Takashi Saito

Report received on Mar. 20, 2020

■**ABSTRACT**■ In the autumn of 1998, Toyota Motor Corporation launched the world's first mass-produced car that adopted a titanium-based composite material for the engine valves. First, this article describes the development of an ultralow-cost manufacturing process for titanium parts, which began at Toyota Central R&D Labs., Inc. in the mid-1980s, and the invention of high-performance titanium-based composite materials using this process. This article then describes the process by which these materials were applied to automotive components in cooperation with Toyota Group companies, and further explains the issues that remain for widespread use of titanium as an automotive material.

■**KEYWORDS**■ Titanium Alloy, Metal Matrix Composites, MMC, TiB, Powder Metallurgy, Blended Elemental Method, Sintering, Automobile, Engine Component, Exhaust Valve, Formula 1

Contents

1. Introduction
2. Issues of Titanium Alloy as an Automotive Material
3. Taking on the Challenge of Developing Low-cost Titanium Components
 - 3.1 Feasibility of Powder Metallurgy
 - 3.2 Density and Pores of Sintered Titanium Alloys
4. Taking on the Challenge of Developing High-performance Sintered Titanium Alloys
 - 4.1 Development of New Process to Increase Density, Reduce Pore Size, and Refine Microstructure
 - 4.2 Special Microstructural Control for Sintered Titanium Alloy
 - 4.3 Improvement of Mechanical Properties by Process and Alloy Composition Refinement
5. Development of High-performance Titanium Metal Matrix Composites (MMC)
 - 5.1 Selection of Optimum Reinforcement Compound for Ti-MMC
 - 5.2 Optimization of Matrix Alloy for TiB Particle Reinforced Ti-MMCs
 - 5.3 Hot Workability of TiB Particle Reinforced Ti-MMCs
6. Development of Ti-MMC Engine Valves for Mass-produced Passenger Vehicle
 - 6.1 Setting of Development Targets
 - 6.2 Extremely Low-cost Manufacturing Process
 - 6.3 Selection of Alloy Composition and Optimization of Heat Treatment Conditions
 - 6.4 Effect of TiB Particle Quantity on Mechanical Properties and Hot Workability
 - 6.5 Durability and Reliability of Ti-MMC Exhaust Valves
 - 6.6 Performance of Ti-MMC as Engine Valves
7. Application of Developed Ti-MMC Valves to Toyota Formula 1 Engine
8. Achieving Further Cost Reductions
 - 8.1 Issues of Mass-produced Ti-MMC Engine Components
 - 8.2 Development of Ultra-high-density Compaction Technology
 - 8.3 Improving Productivity Using Continuous Sintering Furnace
9. Proposal for the General Adoption of Titanium (in Place of a Conclusion)

1. Introduction

Before the development of the materials described in this paper, racing cars had already adopted a wide range of titanium alloy components since titanium alloy reciprocating engine components can operate at much higher rotational speeds than steel. The adoption of titanium was also part of ongoing efforts to reduce the weight of engine valves, one of the main types of such reciprocating components. However, although titanium alloy intake valves had been adopted on some commercial sports cars, none had adopted titanium exhaust valves. Although partly a reflection of the cost of titanium, this was principally due to the lack of a titanium alloy with long-term durability when exposed to high temperature exhaust emissions.

In 1998, twenty-two years ago, Toyota Motor Corporation (abbreviated hereafter as Toyota) launched the Altezza, a mass-produced passenger vehicle installed with the 3S-GE engine, which adopted titanium mono-boride (TiB) particle reinforced titanium metal matrix composites (TiB/Ti-MMC) exhaust valves and sinter-forged titanium alloy intake valves (**Fig. 1**). This TiB/Ti-MMC technology originated at Toyota Central R&D Labs., Inc. (abbreviated hereafter as Toyota CRDL),⁽¹⁻⁶⁾ and was jointly developed and commercialized by the Production Engineering Development Div. at Toyota, Fine Sinter Co., Ltd., and Aisan Industry Co., Ltd.⁽⁷⁻⁹⁾ Nine years later, in 2007, a high-performance variant of this technology was also adopted in Toyota Formula 1 (F1) race car engines⁽¹⁰⁾ with positive results that are still fresh in the mind. This material was subsequently adopted in the engines for the high-performance Lexus LFA sports car (**Fig. 2**),⁽¹¹⁾ which went on limited sale in 2010 and the Lexus RC-F⁽¹²⁾ launched in 2014. In 2000, almost immediately after the launch of the Altezza, Yamaha Motor Co., Ltd. also adopted this material in the engine of the YZ-250F motocross motorcycle, and continues to use it for various motocross models.

This article describes why Toyota decided to adopt titanium for both the intake and the exhaust valves in a mass-produced vehicle rather than a racing car. It also describes why this material has not been adopted on a wider range of vehicles, the remaining challenges to be addressed, as well as potential solutions for these challenges.



Fig. 1 The first mass-produced car in the world to feature TiB/Ti-MMC engine valves.



1LR-GUE



Fig. 2 Appearance of Lexus LFA and its NA 4.8-liter V10 1LR-GUE engine.

2. Issues of Titanium Alloy as an Automotive Material

Figure 3 compares the specific strength (i.e., tensile strength/specific gravity) of a range of typical structural metals. As shown in the figure, the order of specific strength is as follows: normal steel < high-strength aluminum (Al) alloy < high-strength steel < high-strength magnesium (Mg) alloy < Al alloy metal matrix composite (MMC) < Maraging steel < titanium alloy. Therefore, as titanium alloy is known to have higher specific strength than any other practically available metal, it is a widely adopted and indispensable material for reducing weight in many fields, including aviation, space, armaments, racing cars, and sporting goods. Another important property of titanium alloy is its unmatched corrosion resistance. Applications that take advantage of this property include weather resistant building materials, marine vessels, marine structures, as well as cooking and eating utensils. In addition, since titanium has extremely low toxicity for humans, it also plays an irreplaceable role in the medical field for artificial bones, implants, catheters, dental corrective devices, and so on.

However, despite its wide-ranging advantages as a structural metal, the extremely high cost of titanium components has restricted its actual adoption. In terms of the abundance of metals in the Earth's crust, titanium is more abundant by an order of magnitude than chromium (Cr), nickel (Ni), copper (Cu), manganese (Mn), carbon (C), phosphorous (P), sulfur (S),

and only lower in abundance than particularly common metals such as silicon (Si), Al, iron (Fe), and Mg. Despite this, however, there are two reasons why titanium components are so costly. The first is that titanium is highly reactive with oxygen (O) and is not easily reduced. As a result, titanium is difficult to isolate or refine from oxide mineral ores. Another reason is its inferior formability of titanium, as defined in the following terms. First, titanium is difficult to cast due to the extremely high reactivity of molten titanium with melting crucibles and casting dies. Second, titanium has a poor forging workability due to its crystalline structure (hexagonal close-packed) and extremely rapid grain growth rate at an elevated temperature. Finally, titanium is difficult to machining since it has a clear tendency to adhere to and react with cutting tools. The poor formability of titanium causes substantial reductions in material yields and puts further upward pressure on cost. As an example, **Fig. 4** shows photographs of a titanium alloy component (a connecting rod used in a Toyota F1 racing car engine) at different stages of production. On the right is the connecting rod after forging and deburring. The final part after machining is shown on the left. The final machined part weighs approximately 250 g, much less than the approximately 850 g of the as forged part. This means that the machining yield of this component is only around 30%. Machining yields are even lower for aircraft parts and other components that require complex shapes, and it is not unusual for these yields to fall below 10%.

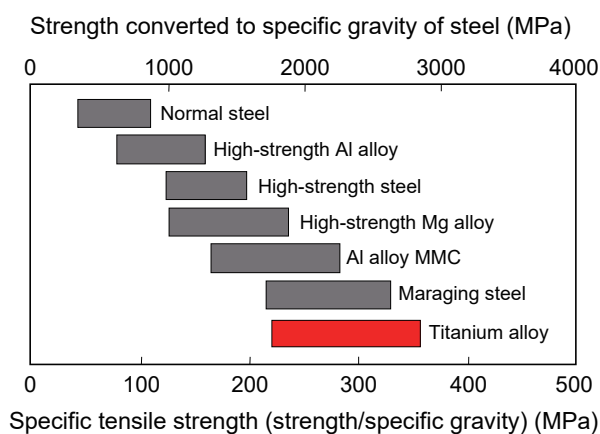


Fig. 3 Comparison of specific strength (tensile strength/specific gravity) of various structural metals.



Fig. 4 Titanium alloy (SP-700) connecting rod for Toyota F1 engine (left) machined from hot forged preform (right).

Overcoming this cost barrier was the first issue to be resolved before titanium alloy could be adopted for the moving parts of mass-produced vehicles. In addition, despite the overwhelming advantage of titanium alloy in terms of specific strength compared to conventional steel, this advantage actually created several issues for the application of titanium alloy to moving parts in a vehicle. The first is the issue of stiffness. The specific stiffness (i.e., Young's modulus/specific gravity) of all structural metals (iron, titanium alloys, aluminum alloys, magnesium alloys, copper alloys, and the like) is coincidentally around 25 GPa/cc/g. This means that achieving a substantial reduction in weight through material substitution is not a principal aim for components that prioritize stiffness over strength as a design criterion. The second is the issue of wear resistance. To a varying degree, excellent sliding characteristics are a requirement of engine components. However, titanium alloy has lower wear resistance than steel and no low-cost surface treatment technologies were available. The third is the issue of heat resistance. Although titanium alloys have higher heat resistance than aluminum and magnesium alloys, no heat-resistant titanium alloys had been developed with superior high-temperature properties to the heat-resistant steel generally adopted in vehicle exhaust systems.

Consequently, two objectives had to be realized before titanium alloy could be adopted in mass-produced vehicle components. The first objective was to reduce manufacturing costs to a level comparable to conventional steel (i.e., the cost of the raw material, forming processes, machining yield, surface refinements, and so on). The second objective was to drastically improve material characteristics other than specific strength (such as specific stiffness, wear resistance, and heat resistance). Unless both objectives could be realized at the same time, titanium alloy could not be considered as a replacement for conventional steel components in mass-produced vehicles.

3. Taking on the Challenge of Developing Low-cost Titanium Components⁽¹³⁻¹⁵⁾

3.1 Feasibility of Powder Metallurgy

The previous section outlined the reasons for the high cost of titanium alloy components. It was realized that drastic cost improvements could not be achieved without making fundamental changes. First,

to address the raw material cost, one issue was to identify the maximum limit of impurities that could be permitted in the raw material without adversely affecting the material properties. Second, to achieve far-reaching improvements in material yield, it was necessary to take on the challenge of adopting low-cost net shaping technology. The final issue was the development of low-cost surface treatment and machining technologies. At the same time, to help realize these dramatic improvements in manufacturing technologies, the research team also understood the necessity of developing more refined alloy composition and microstructure control techniques suitable for industrial processes.

Research focused on powder metallurgy to accomplish these objectives. Powder metallurgy is a production method in which metal powder is molded by compression in a die and then sintered at high-temperature. It started to attract a great deal of attention in the 1970s as a low-cost forming technology for steel components, and was already in use for automotive parts. Toyota CRDL began studying the applicability of titanium alloy vehicle components in the mid 1980s. At the time, research into titanium powder metallurgy had begun in the U.S., primarily for military applications.⁽¹⁶⁻¹⁸⁾ Two main technological approaches were in practical use around the world. The first was the alloy powder method. In this method, titanium alloy powder with the target chemical composition is fabricated in advance by gas atomizing⁽¹⁸⁾ or via the rotating electrode process (REP).⁽¹⁹⁾ The powder is then enclosed in a metallic can and densified by hot isostatic pressing (HIP).⁽²⁰⁾ The second was the blended elemental (B/E) method.⁽²¹⁾ In this method, pure titanium powder is mixed with a master alloy powder selected to reinforce the material, before being pressed into the shape of the component in a metallic die and densified by vacuum sintering.

In addition to the high cost of fabricating the alloy powder and the HIP process, the material yield of the alloy powder method was also extremely low because net shaping techniques could not be adopted. Despite the lack of any cost advantage over conventional forging technology, it attracted attention as a way of forming high-performance titanium alloys with a uniform composition and microstructure. In contrast, the B/E method involved the blending of low-cost pure titanium powders (such as sponge fine or

hydride-dehydride (HDH) powder) with low-cost master alloy powders (primarily pulverized powders). The resulting blended powder is compacted into the product shape in a metallic die and further densified by vacuum sintering. This process directly allows the manufacture of near net shape components and is a far lower-cost technique than ingot forging or the alloy powder method. However, as evidenced by the expression “cheap and nasty”, components manufactured by the B/E method have far inferior material properties to forged components. In particular, one fatal issue of components manufactured by the B/E method compared to ingot forged components is extremely low fatigue strength, a very important material property under practical usage conditions.⁽²²⁾ **Figure 5** compares the fatigue properties of a typical titanium alloy (Ti-6Al-4V: mass%) manufactured by the B/E method (○, ◇) with the same alloy manufactured by sintering and HIP (□) after a tensile/compression fatigue test (stress ratio $R = 0.1$). The reasons why the B/E method was not regarded as reliable are obvious: first, the properties of sintered materials fabricated by the B/E method differ widely depending on the raw material powder. Then, there is a clear difference between these alloys and the alloy after HIP (□). It should also be noted that the fatigue properties of a sintered titanium alloy after HIP are comparable to those of an ingot forged material.⁽¹⁷⁾

Therefore, Toyota CRDL began research in the mid 1980s motivated by the idea of utilizing the cost

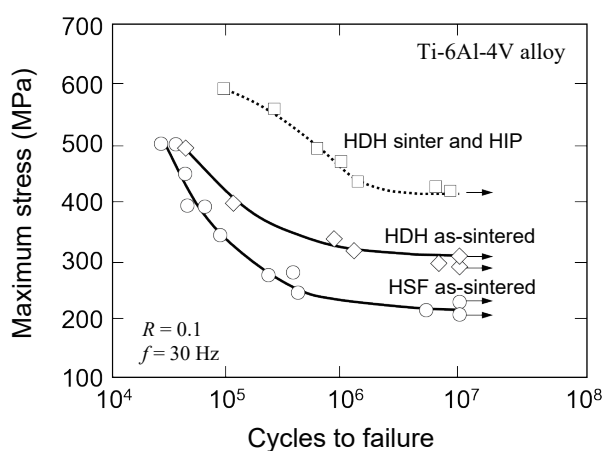


Fig. 5 Comparison of fatigue properties of B/E as-sintered Ti-6Al-4V alloy using different type of titanium powders and post sinter HIP'ing.

advantage of the B/E method while finding a way to improve fatigue properties. It was felt that this might enable the development of a usable titanium alloy for mass-produced automotive components. The inferior fatigue properties of sintered titanium alloys manufactured by the B/E method are due to the notching effect of pores in the sintered titanium alloy. Therefore, it was initially posited that this material could not be used to manufacture important components unless these pores could be eliminated by applying HIP to the sintered product.⁽¹⁷⁾ However, there was a total lack of fundamental research into this matter. No reports described the sizes of pores in sintered titanium alloys and to what extent these pores affected fatigue strength. Therefore, Toyota CRDL started its research by examining why sintered materials have low fatigue strength.

3.2 Density and Pores of Sintered Titanium Alloys

Figure 6 shows the microstructure of a typical sintered titanium alloy (Ti-6Al-4V) manufactured using different types of powder. The titanium powder used for the alloy shown in Fig. 6(a) is low-cost Hunter sponge fine (HSF) powder with a high impurity

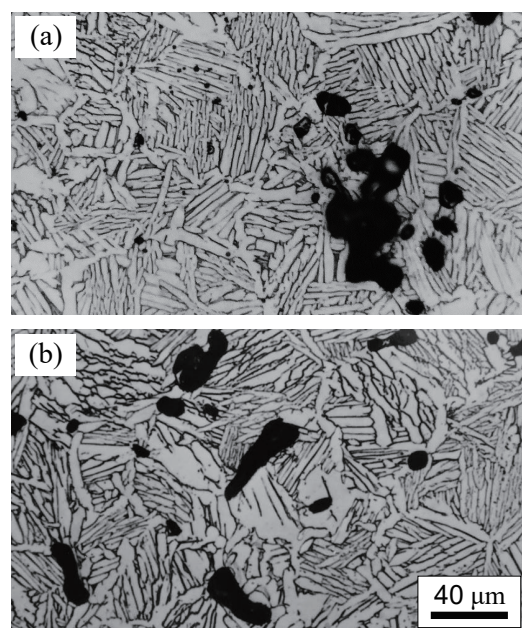


Fig. 6 Change in sintered microstructure of Ti-6Al-4V alloys using different type of titanium powders: (a) HSF powder and (b) HDH powder.

content. In comparison, the titanium powder used for the alloy shown in Fig. 6(b) is HDH powder, a relatively high-cost powder with a lower impurity content. Both were compacted under a pressure of 392 MPa in a metallic die and vacuum sintered at 1300°C for four hours. Although both sintered compacts have a density of approximately 97% with respect to the true density, the distribution and pattern of the pores are completely different. With the HSF powder, the distribution of pores is uneven and pore size is irregular. In Fig. 5, the fatigue properties of the HDH powder component are shown by the \diamond symbols and the fatigue properties of the HSF powder component are shown by the \circ symbols. These results indicate that the size and distribution of pores have a major effect on fatigue properties. It also shows that the fatigue properties of even a high-cost HDH powder component with this density and pore distribution cannot approach those of a regular forging or a sintered alloy manufactured by the alloy powder method.

Therefore, this research took on the challenge of using low-cost HSF powder to create an alloy structure with pores that are as uniform and finely distributed as possible. **Table 1** compares the chemical analysis results and price (in 1985 U.S. dollars) of HSF and HDH powders. The following three major differences are evident: (1) HSF powder is clearly less expensive than HDH powder, (2) HSF has a higher sodium and chlorine content than HDH powder, and (3) the oxygen content of HSF powder is approximately half that of HDH powder. These differences are caused by the powder manufacturing process and can be explained simply as follows.

First, HSF powder is a by-product of the Hunter method (a sodium reduction method) used to manufacture sponge titanium, and is a fine powder with very few alternative uses. For this reason, the price of HSF powder is very low and it contains little oxygen because it is a form of sponge titanium. However, since the Hunter method involves reducing titanium tetrachloride using metallic sodium, large quantities of sodium chloride (NaCl) are generated that have to be washed off by water. As a result, HSF powder unavoidably contains some residual NaCl. **Figure 7** shows a photograph of particles (mainly NaCl and ferric oxide (Fe_2O_3)) sieved out of commercially available HSF powder. In contrast, HDH powder is fabricated as follows. First, sponge titanium manufactured by the Kroll method (a magnesium reduction method)

Table 1 Chemical analysis of applied titanium powders.

Powder	O	Cl	Na	Mg	Fe	Ti	Price (U.S. \$/kg)
HSF	0.11	0.08	0.078	---	0.02	99.6	5 to 10
HDH	0.19	<0.002	---	<0.001	0.029	99.8	20 to 50

is embrittled by hydrogenation. The powder is then fabricated by grinding at room temperature before a further vacuum dehydrogenation treatment at around 500°C. Unlike the Hunter method, the final vacuum treatment of the Kroll method is capable of removing the magnesium chloride (MgCl_2) by-product generated during refining. Therefore, the amount of residual chlorides is extremely low even without washing. However, the multiple heat treatments required to manufacture this powder push up the manufacturing cost and generate a relatively high oxygen content. **Figure 8** shows scanning electron microscope (SEM) images comparing the appearance of HSF and HDH powders. The HSF powder shares the distinctive irregular appearance of sponge titanium, whereas the HDH powder has the distinctive squarish clumps associated with crushed powders.

The graph in **Fig. 9** compares the tap, green, and sintered densities of a titanium alloy manufactured using HSF and HDH powders. Since HSF powder has lower flowability than the HDH powder, its tap density is also substantially lower. In contrast, since HSF powder is easily plastic deformed due to its lower oxygen content, its green density is higher. However, since the density of HSF powder is less easy to increase by sintering, the final density of both powders is roughly the same (approximately 97%). The poor sintering properties of HSF powder materials is because the NaCl particles included in the powder do not melt into the titanium during sintering and become trapped between the titanium particles, hampering the sintering shrinking process. It is thought that the large pores exceeding 100 μm shown in Fig. 6(a) are caused by these NaCl particles.

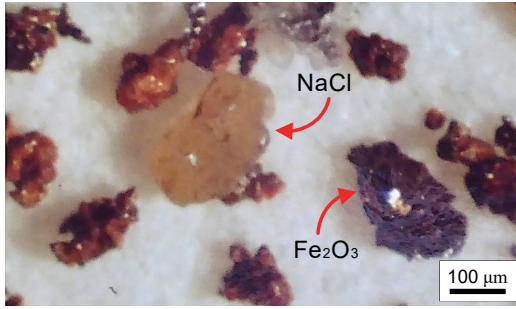


Fig. 7 Inclusion particles extracted from the HSF titanium powder.

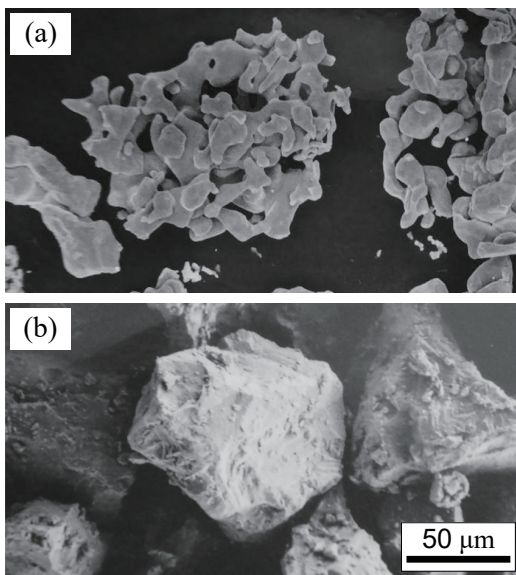


Fig. 8 Appearance of (a) HSF and (b) HDH titanium powders (#150).

Titanium powders: #150, Compacting: 392 MPa, Sintering: 1300°C for 4 hours

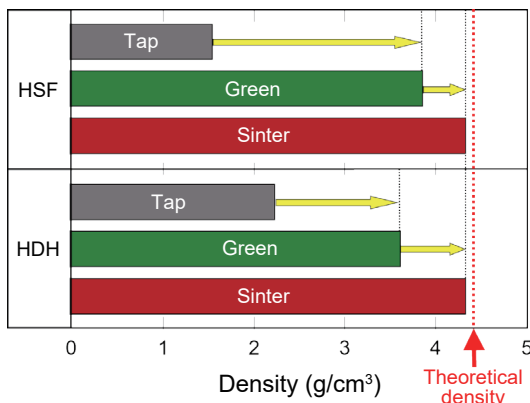


Fig. 9 Comparison of tap, green, and sintered densities of Ti-6Al-4V alloy manufactured by conventional B/E method using different type of titanium powders.

4. Taking on the Challenge of Developing High-performance Sintered Titanium Alloys

4.1 Development of New Process to Increase Density, Reduce Pore Size, and Refine Microstructure

The large pores that remain in sintered bodies manufactured by low-cost HSF powder are thought to be caused by the intrusion of large NaCl particles. Based on this presumed mechanism, reducing the size of these NaCl particles was thought to be a way of eliminating large pores. Therefore, a kneading process using a high-energy ball mill was adopted to crush the NaCl particles included in the titanium powder. Since finer master alloy powders are known to promote the sintering of titanium alloy, the high-energy ball mill was used first to finely crush the master alloy. The HSF powder was then introduced into the mill to blend the materials within a short time frame while also kneading the titanium powder. **Figure 10** shows the appearance of the HSF powder after kneading treatment. Compared to the HSF powder before kneading as shown in Fig. 8, the kneaded HSF powder appears as rounded clumps. The large NaCl particles have been broken up and are adhered on the surface of the titanium powder as fine particles alongside the master alloy powder. The kneading treatment substantially improved the flowability of the powder, thereby raising the tap density of the powder 1.5 times higher than that of non-treated powder.

Figure 11 shows the sintered microstructure of Ti-6Al-4V alloys manufactured using the new mixing with kneading process. Regardless of the type of titanium powder, both the quantity and size of the pores were drastically reduced under the same compacting and sintering conditions compared with the conventionally manufactured alloys shown in Fig. 6, and a relative density of 99% was achieved. This figure clearly indicates the effect of the powder mixing process on the titanium alloy microstructure. Specifically, in the case of the titanium alloy manufactured using HSF powder, since NaCl never dissolve into the titanium alloy at elevated temperature, NaCl particles pulverized by the kneading treatment are stably dispersed in the titanium matrix during sintering process showing an important effect of pinning the β phase grain boundaries. This pinning effect suppresses β phase grain growth and changes the acicular α phase inside the β grain structure to granular

α phase. In contrast, since there is no pinning effect of included particles using HDH powder, β phase grains grow significantly with densification during sintering, which forms a coarser acicular α phase inside the β grain structure during cooling stage.

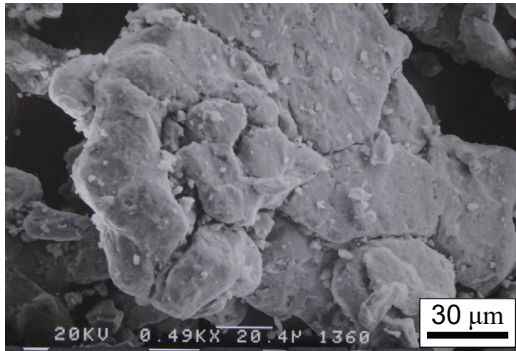


Fig. 10 Surface morphology of HSF powder after kneading.

4.2 Special Microstructural Control for Sintered Titanium Alloy

As shown in Figs. 6 and 11, ($\alpha + \beta$) type titanium alloys as typified by Ti-6Al-4V form a rough acicular ($\alpha + \beta$) microstructure if slowly cooled from the sintering temperature (i.e., the stable β phase region). Since this type of directionally aligned coarse acicular microstructure has an adverse effect on mechanical properties such as fatigue and ductility, a further heat treatment is generally required to adjust the microstructure. However, to avoid a costly post-sintering heat treatment, it is necessary to create a fine uniform microstructure through the slowly cooling conditions after sintering.

An important aspect of creating a finer microstructure through slowly cooling is to delay the transformation from the β to the α state. This can be accomplished by lowering the β to α transition temperature (i.e., stabilizing β phase). An effective means of achieving this objective is to add a β stabilizing element having small diffusivity in β titanium. After analyzing the diffusion coefficients of elements in β titanium,⁽²³⁾ it

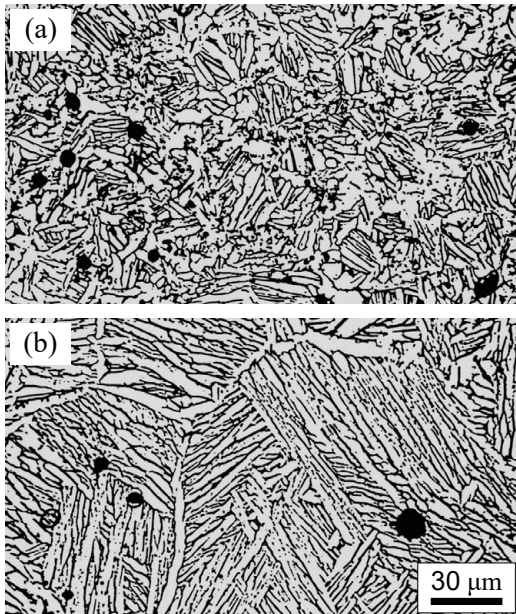


Fig. 11 Change in sintered microstructure of Ti-6Al-4V alloys using new mixing process and different titanium powders: (a) HSF and (b) HDH. The sample preparation conditions were the same as the alloys shown in Fig. 6.

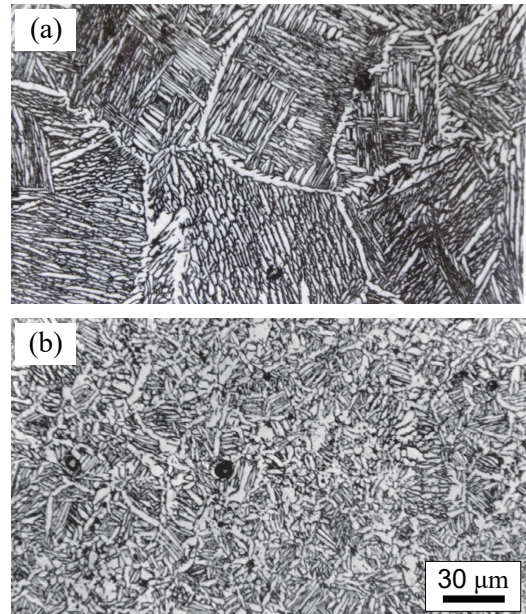


Fig. 12 Effect of Mo and B addition on the microstructure of HDH Ti-6Al-4V alloy: (a) Ti-6Al-4V-1Mo and (b) Ti-6Al-4V-1Mo-0.3B. Other conditions are the same.

Table 2 Comparison of impurity diffusivity of several β -stabilizing elements in β -titanium at 900°C, normalized by the self-diffusivity of titanium.

Element	Ni	Co	Fe	Mn	Cr	Ti	V	Nb	Mo
Diffusivity	56	42	18	4.9	1.8	1	0.7	0.6	0.2

was proposed that the addition of molybdenum (Mo), an element with a particularly low diffusion coefficient in β titanium, would be most effective (**Table 2**). As predicted, the addition of a small amount of Mo was extremely effective in creating a fine acicular α phase microstructure (**Fig. 12**). However, it was found that adding Mo facilitated the precipitation of network-like α phase structures along the β phase grain boundaries during cooling (**Fig. 12(a)**). In response, dispersing the fine precipitates that inhibit β phase grain growth was proposed as an effective way of suppressing α phase precipitation along the grain boundaries. Consequently, the research team searched for a particle additive with low mutual solubility with titanium that would not dissolve into β titanium even at high temperatures. As a result, several candidate additives were identified that effectively suppressed abnormal grain growth during sintering and formed equiaxed acicular α phases, including NaCl (described above), yttrium oxide (Y_2O_3), yttrium chloride (YCl_3), and boron (B). As a typical example, **Fig. 12(b)** shows the microstructure of a sintered Ti-6Al-4V alloy containing small amounts of both Mo and B after slowly cooling. The fine acicular α phases created by the addition of Mo were equiaxed by the co-addition of B. The network-like α phase structures along the grain boundaries have disappeared and an extremely fine and uniform equiaxed structure has been formed. The noteworthy phenomenon here is that the B additive is dispersed as fine TiB grains with stable thermodynamic properties within titanium alloys. It is thought that these finely dispersed TiB particles help to prevent coarsening of the β phase crystalline grains during sintering and act as nuclei for α phase precipitation during cooling, thereby promoting the formation of an equiaxed fine $\alpha + \beta$ structure. This discovery was a major hint for titanium-based composite material development in the future.

4.3 Improvement of Mechanical Properties by Process and Alloy Composition Refinement

Table 3 compares the sintered density, maximum pore size, and tensile properties of typical Ti-6Al-4V sintered alloys manufactured using HSF or HDH powder with two different master alloy powder sizes (9 and 40 μm in average diameter), with and without kneading treatment, and with and without the addition of elements to refine the microstructure (Mo + B). **Figure 13** compares the fatigue properties of the six samples (A to F) shown in **Table 3**.

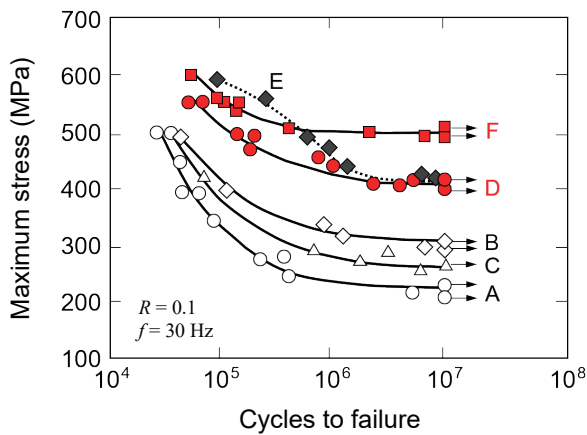
To summarize the results, kneading the powder enabled static and fatigue strength properties equivalent to a titanium alloy manufactured using high-cost HDH titanium powder and HIP, even when low-cost HSF titanium powder was used. Based on these results, it was found that a maximum pore diameter of less than 20 μm would not have an adverse effect on fatigue properties. In addition, combining kneading with the addition of elements to refine the microstructure enabled substantially improved mechanical properties compared to those achieved by HIP using high-purity (expensive) HDH titanium powder, even when as-sintered condition using low-purity (cheap) HSF titanium powder.

In conclusion, it was found that even the low-cost B/E method could be used to easily achieve material properties equal in every way to high-cost conventional forged materials by improving the powder treatment and additive minor alloying elements. However, as described in the introduction, this performance was still insufficient to enable the application of titanium alloys to automotive structural materials, and further performance gains were required. Therefore, the focus of the research switched to the development of a low-cost and high-performance titanium-based composite material.

Table 3 Comparison of static mechanical properties of B/E titanium alloys and manufacturing conditions.

Common conditions: titanium powder size = #150, compacting at 392 MPa, sintering at 1300°C for 4 hours

Sample	Titanium powder	Powder treat.	Al ₃ V powder (μm)	Sintered density (%)	Max. pore size (μm)	Tensile strength (MPa)	Tensile elongation (%)	Alloy composition
A	HSF	None	40	96.5	150	840	3.7	Ti-6Al-4V
B	HDH	None	40	97.0	60	870	14.5	Ti-6Al-4V
C	HSF	None	9	99.1	100	923	6.3	Ti-6Al-4V
D	HSF	Kneading	9	99.2	20	922	15.0	Ti-6Al-4V
E	HDH	None	40	100.0 (HIP)	0	945	17.0	Ti-6Al-4V
F	HSF	Kneading	9	99.5	10	1010	12.5	Ti-6Al-4V-1Mo-0.3B

**Fig. 13** Comparison of fatigue properties of blended elemental Ti-6Al-4V alloys prepared under the various conditions listed in Table 3.

5. Development of High-performance Titanium Metal Matrix Composites (MMC)⁽¹⁻⁶⁾

5.1 Selection of Optimum Reinforcement Compound for Ti-MMC

Assuming application of the B/E method with high-temperature sintering, the conditions for an ideal reinforcement compound for titanium alloy include the following: (1) high strength, hardness, heat resistance, and stiffness, (2) remarkable thermodynamic stability in titanium alloys throughout the temperature range, (3) constituent elements of the compounds never soluble into the titanium matrix, (4) difference in thermal expansion coefficient between the titanium matrix and the reinforcement compound is small, and

(5) high bonding strength between the titanium matrix and reinforcement compound. However, at the time (the second half of the 1980s), all the reinforcement compounds for titanium-based composite materials that were being researched primarily in the U.S. (such as titanium carbide (TiC), silicon carbide (SiC), titanium nitride (TiN), titanium diboride (TiB₂), silicon nitride (Si₃N₄), boron carbide (B₄C), alumina (Al₂O₃), and so on) either resulted in low thermodynamic stability in the titanium alloy, or were fundamentally unsuitable for use as a reinforcement compound due to mutual large solubility between the titanium matrix and the compounds. Such research was attempting to boost performance through the suppression of interface reactions by, for example, modifying the interfaces between the reinforcement compound and titanium matrix.⁽²⁴⁾

In contrast, the research at Toyota CRDL had focused on the dispersing of TiB compound particles. The advantage of this compound compared to the reinforcement compounds listed above in terms of thermodynamic properties can be easily imagined from the Ti-B phase diagram shown in **Fig. 14**. Specifically, the boron forms virtually no solid solution with the titanium matrix in a range from room temperature up to just below the melting point. In addition, the TiB phase forms a stoichiometric compound with a Ti:B ratio of 50:50, which means that it has virtually no solid solubility. This strongly suggests that TiB particles in a titanium alloy would be extremely thermodynamically stable and have no adverse effects on the mechanical properties of the titanium matrix. Furthermore, as shown in **Table 4**, TiB has extremely high strength and elastic modulus, as well as virtually the same coefficient of linear thermal expansion as titanium

alloys. As a result, TiB has the ideal properties for use as a titanium alloy reinforcement compound.

Based on the previous analysis, the research team

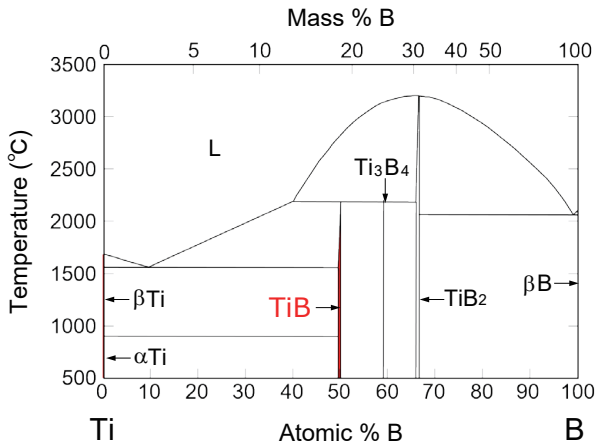


Fig. 14 Phase diagram of Ti-B binary system.

was sure that using TiB as a reinforcement compound for titanium alloys manufactured using the B/E method could achieve dramatic improvements in material properties. Although stable when present in titanium alloy, TiB itself is an unstable compound and cannot be obtained in powder form. However, stable TiB particles can be created from various boride powders by recombining the boron atoms in the boride with titanium atoms, which have a stronger chemical affinity, in the sintering process. **Figure 15** shows microstructural images of an alloy (10 vol% TiB/Ti-6Al-4V) manufactured using HSF titanium powder, Al-40 mass%V master alloy powder, and TiB_2 powder stirred and mixed together in a high-energy ball mill, compacted in a metal die at 392 MPa, and vacuum sintered at 1300°C for 16 hours. Figure 15(a) shows that the squared-off TiB particles are dispersed uniformly, the enlarged image in Fig. 15(b) shows that the interfaces between the TiB particles and matrix

Table 4 Adaptability of reinforcement compounds for titanium matrix composites.

Compound	Knoop hardness (GPa)	Young's modulus (GPa)	Coefficient of linear expansion ($\times 10^{-6} \text{K}^{-1}$)	Maximum solubility (atomic%)		Estimation
				[Matrix]	[Particle]	
TiB	28.0	550	8.6	< 0.001	1.0	Excellent
TiC	24.7	460	7.4	1.2	15.0	Passable
TiN	24.0	250	9.3	22.0	26.0	Unacceptable
SiC	25.0	420	4.3	Unstable in Ti alloy		Unacceptable
Si_3N_4	14.7	320	3.2	Unstable in Ti alloy		Unacceptable
TiB_2	34.0	529	6.4	Unstable in Ti alloy		Unacceptable
B_4C	27.5	449	4.5	Unstable in Ti alloy		Unacceptable
Al_2O_3	22.5	350	8.1	Unstable in Ti alloy		Unacceptable

The coefficient of linear expansion of titanium alloy is around $9.0 \times 10^{-6} \text{K}^{-1}$

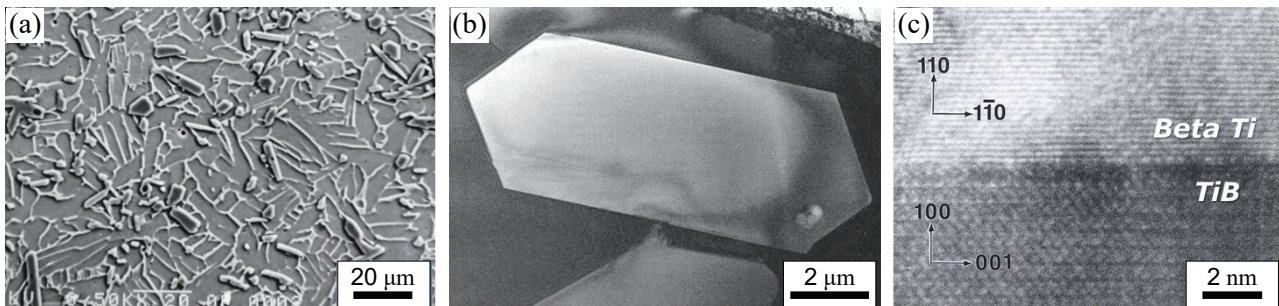


Fig. 15 Microstructure of B/E 10 vol% TiB/Ti-6Al-4V MMC: (a) macro image (SEM), (b) TiB particle (TEM) and (c) TiB/b Ti interface (TEM).

alloy are linear, and the lattice image in Fig. 15(c) shows that the β titanium matrix/TiB particle interface is extremely consistent. **Figure 16** compares the fatigue properties of a Ti-6Al-4V sintered alloy manufactured by the new process using HSF titanium powder and an MMC containing 10 vol% of TiB in a Ti-6Al-4V alloy. These results illustrate the dramatic improvement in fatigue properties achieved by dispersing TiB particles into the titanium alloy. For normal metallic materials, it is relatively simple to improve static strength, stiffness, wear resistance and the like by composite particle dispersing. However, fatigue properties and impact characteristics are regarded as particularly difficult to improve by the same method due to the insufficient bonding strength of the interface between the matrix alloy and reinforcement compound. These interfaces are susceptible to becoming the origin point of fatigue fractures due to concentrations in stress. Fractures that occur are also likely to propagate along these interfaces. However, it was estimated that the significant improvement in fatigue properties was due to reasons such as the extremely high consistency and strong bonding of the TiB particle/titanium alloy matrix interface (Fig. 15(c)) and the almost identical coefficients of thermal expansion of the both constituent materials (Table 4). These results verified that TiB is the ideal reinforcement compound for titanium alloy.

5.2 Optimization of Matrix Alloy for TiB Particle Reinforced Ti-MMCs

The data shown in Fig. 16 was obtained based on a Ti-6Al-4V alloy. However, one of the advantages of the B/E method is the capability to freely alter the composition of the matrix alloy by adjusting the master alloy powder. **Table 5** shows the combinations of master alloy powders adopted to manufacture various titanium alloys for trial. The compositions of the analyzed master alloys were selected based on grindability. Some of the combinations included pure metallic powders. For example, Ti-6Al-4V and Ti-3Al-2V alloys were analyzed as ($\alpha + \beta$) type MMCs with a good balance of strength and stiffness. In addition, presuming the application of the material to the manufacture of connecting rods, an extremely strong β type Ti-7Mo-4.5Fe-1.5Al-1.5V alloy MMC for forging was also studied.⁽²⁵⁾

Figure 17 compares various mechanical properties

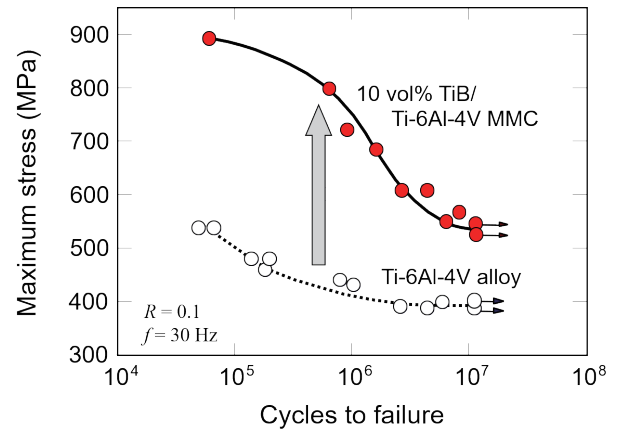


Fig. 16 Increase in fatigue strength of Ti-6Al-4V sintered alloy by addition of 10 vol% TiB particles obtained by the new B/E process.

Table 5 Combinations of master alloy compounds for manufacturing B/E titanium alloys.

Target titanium alloy composition	Combinations of master alloy compounds
Ti-6Al-4V, Ti-3Al-2V	Al-40V
Ti-6Al-4V-1Mo-0.2B	Al-40V + pure Mo + TiB ₂
Ti-8Al-1Mo-1V	Al-38Ti + Al-40V + pure Mo
Ti-6Al-2Sn-4Zr-2Mo-0.2Si	Al-14Sn-28Zr-1.4Mo-1.4Si
Ti-6.5Al-4.5Sn-4.5Zr-1Nb-1Mo-0.35Si	Al-25Sn-25Zr-5.6Nb-5.6Mo-1.9Si
Ti-5Al-12Cr-3.3V	Al-40V + pure Cr
Ti-10V-2Fe-3Al	Al-40V + Fe-80V (ferro-V)
Ti-4.5Fe-7.0Mo-1.5Al-1.5V	Al-50V + Fe-62Mo (ferro-Mo)
Ti-33.5Al	Al-38Ti

of sinter-forged 20 vol% TiB/Ti-7Mo-4Fe-1.5Al-1.5V MMC with those of B/E Ti-6Al-4V sintered alloy. The static and fatigue strength of the MMC are twice as high as the conventional alloy. The Young's modulus of the MMC is also around 1.5 times higher at 160 GPa and the wear resistance is also extremely high.

The research also studied a (near- α) type Ti-6Al-4.5Sn-4.5Zr-1Mo-1Nb-0.3Si alloy MMC to maximize heat resistance for application as engine exhaust valves. Although 650°C was conventionally regarded as the limit of heat resistance for the best heat resistant titanium alloy, this material demonstrated superior fatigue properties to heat-resistant steel at 850°C (**Fig. 18**).

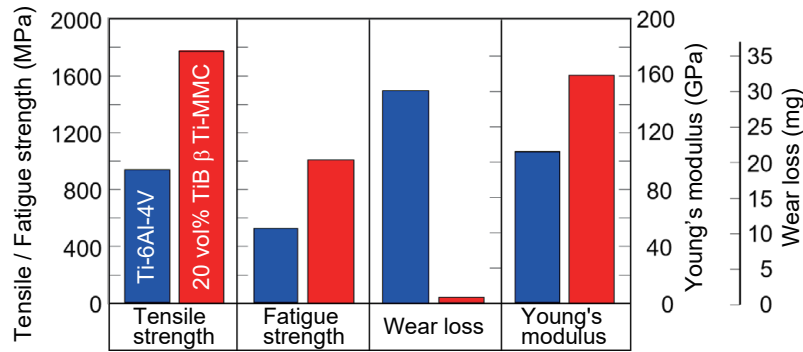


Fig. 17 Comparison of mechanical properties of 20 vol% TiB reinforced β Ti-MMC with conventional Ti-6Al-4V alloy.

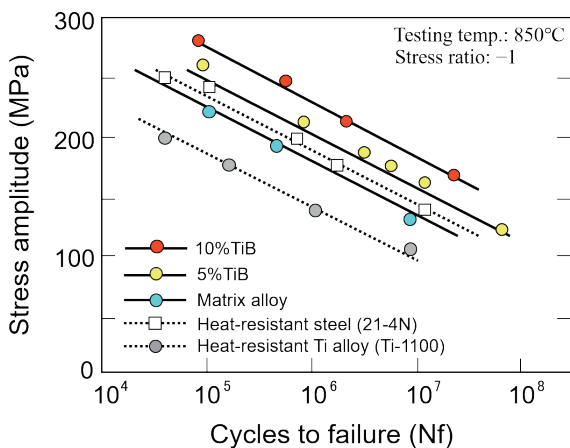


Fig. 18 Effect of TiB particle content on fatigue strength at 850°C of the developed TiB/Ti-6.6Al-4.6Sn-4.6Zr-0.9Nb-1.0Mo-0.35Si MMC.

5.3 Hot Workability of TiB Particle Reinforced Ti-MMCs⁽²⁵⁾

Normally, titanium alloys have a crystal structure of hexagonal close-packed (HCP) α phase at close to room temperature, which transforms into a body centered cubic (BCC) β phase at high temperatures. This β phase has a high self-diffusion coefficient and generates rapid grain growth. Therefore, if the titanium alloy is heated above the β transus temperature, the crystal grains become coarser instantly and the titanium alloy becomes susceptible to forging cracks. For this reason, forging has to be carried out in the relatively low

($\alpha + \beta$) dual phase temperature region, which has high deformation resistance. However, if grain growth can be suppressed even after heating the titanium alloy at the single β phase region, forging can be carried out at ultra-high temperatures with low deformation resistance and high deformability. This would also have synergistic effects such as enabling net shaping (thereby improving material yield and minimizing the requirement for machining) and extending the lifetime of the forging dies, helping to achieve major reductions in processing costs.

Figure 19 compares the hot deformability of (a) ($\alpha + \beta$) type Ti-6Al-4V alloy, (b) β type Ti-7Mo-4.5Fe-1.5Al-1.5V alloy, and (c) 20 vol% TiB/Ti-7Mo-4.5Fe-1.5Al-1.5V MMC. To illustrate these results, **Fig. 20** shows side view images of cylindrical test specimens after 75% compression (upset forging) at 800°C. The β phase grains of the Ti-6Al-4V alloy (a), which contains no reinforcing particles, became significantly larger due to the 1300°C sintering process and formed a coarse ($\alpha + \beta$) microstructure in the cooling process after sintering. As a result, this alloy has large deformation resistance and extremely low deformability, which explains the cracks in the sides of the specimen formed at a lower compression range. In contrast, the single β phase microstructure of the β type alloy (b) and the β type alloy matrix MMC (c) at the process temperature (800°C) resulted in substantially lower deformation resistance and higher deformability than the ($\alpha + \beta$) type Ti-6Al-4V alloy. In particular, although the MMC (c) contains 20 vol% of TiB particles, its deformation resistance was virtually identical to the matrix alloy (b).

Furthermore, the extreme smoothness of the side view of the specimen suggests that the deformability of the MMC is even superior to the matrix alloy.

Figure 21 compares the microstructure of the β type matrix alloy and the 20 vol% TiB MMC before hot working. The figure shows that β grain growth has been suppressed by the pinning effect of the TiB particles, which are dispersed in large quantities throughout the microstructure. These results demonstrate that

the dispersing of TiB particles enable hot working in the ultra-high-temperature β region, which had been considered unrealistic for conventional titanium alloys up to that point. **Figure 22** shows an image of a connecting rod formed by one-heat-forging in air at temperatures of 1200°C or higher using a bar-shaped sintered blank manufactured from the 20 vol% TiB/Ti-7Mo-4.5Fe-1.5Al-1.5V MMC. Regardless of the high TiB particle content, an extremely thin and

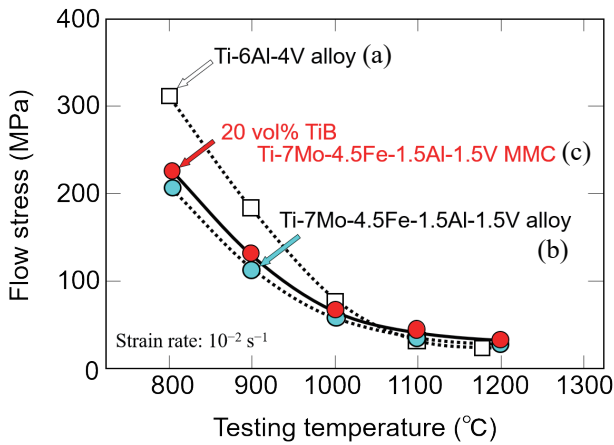


Fig. 19 Change in hot deformability of β Ti-7Mo-4.5Fe-1.5Al-1.5V alloy by addition of 20 vol% TiB particles compared with $\alpha + \beta$ Ti-6Al-4V alloy.

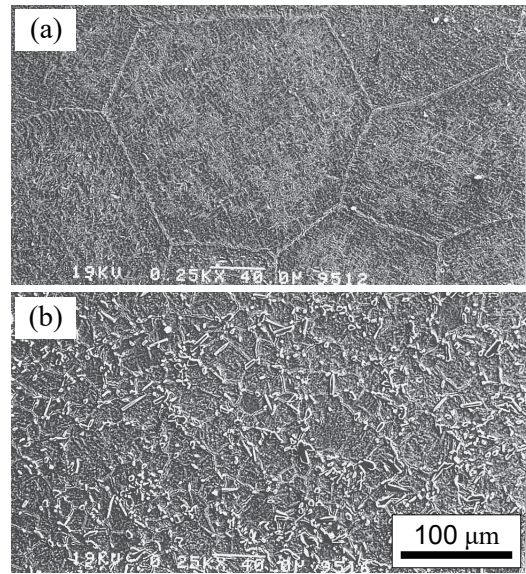


Fig. 21 Pinning effect of the TiB particle on the β grain growth during sintering. (a) β matrix alloy, (b) 20 vol% TiB MMC.

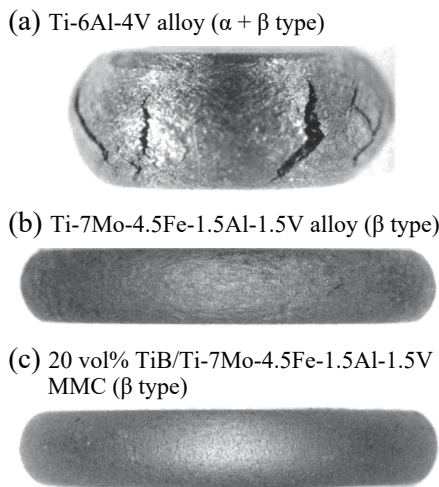


Fig. 20 Side view of upset forging test specimens compressed at 800°C: (a) Ti-6Al-4V alloy, (b) β Ti matrix alloy, and (c) 20 vol% TiB MMC.

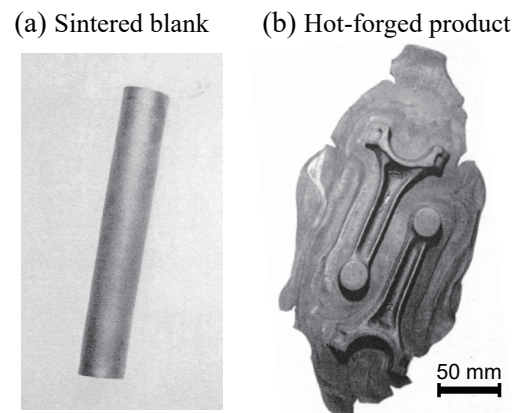


Fig. 22 Connecting rod formed by one-heat-forging at 1200°C using sintered 20 vol% TiB/Ti-7Mo-4.5Fe-1.5Al-1.5V β -Ti MMC.

clean flash has been formed by the hot forging process without cracking, demonstrating the extremely high hot workability of this MMC. The fact that dispersing TiB particles in the titanium alloy actually improved hot workability, rather than having an adverse effect as might be expected, was a particularly noteworthy discovery. As described in the following section, this characteristic became a decisive advantage when applying TiB/Ti-MMC to manufacture valves.

In conclusion, the developed TiB particle reinforced Ti-MMC manufactured using the B/E method was found to have the potential for commercialization at a much lower cost and with clearly superior material characteristics to conventional titanium alloys.

6. Development of Ti-MMC Engine Valves^(7-9,26)

6.1 Setting of Development Targets

Engine intake valve has the minimum cost hurdle among reciprocating engine parts for the application of titanium alloy to mass-produced vehicle. Although intake valves were the most likely candidate, exhaust valves were also regarded as potentially viable, providing the newly developed Ti-MMC could be adapted for mass production. Therefore, a feasibility study was conducted in 1991 with the aim of simultaneously developing both intake and exhaust valves. The target engine was a naturally aspirated (NA) 4-cylinder 2000 cc engine for sporty vehicles, which was due to start production in the second half of the 1990s. The vehicle was positioned as a potential rival to a 2000 cc class high-performance sports car from Honda Motor Co. Ltd. (Honda) that was rumored to be due for release in the near future (the car that became the Honda S-2000). Since it was expected that Honda would develop an ultra-high revving short-stroke NA engine using its variable valve timing & lift electronic

control (VTEC) technology, Toyota began work on an engine with a rev limit of around 8500 to 9000 rpm that could match the expected performance of Honda's engine. To realize this type of ultra-high revving engine, it was absolutely necessary to substantially reduce the weight of the valves. However, since only a minimum increase in costs could be tolerated to manufacture these lightweight valves, it was not possible to greatly exceed the cost of the current heat-resistant steel valves. For these reasons, the engine design division was very keen to use titanium valves if the manufacturing cost could be kept sufficiently low. Development started with this mission.

The manufacturing cost of heat-resistant steel engine valves was between 150 and 350 yen (JPY) per valve. In comparison, the cost of existing titanium alloy intake valves well exceeded 1000 yen (JPY) per valve. In addition, heat-resistant titanium alloy had never been developed anywhere in the world to manufacture exhaust valves in a mass-produced engine. Therefore, the aim of this development was to develop high-performance titanium valves with sufficient potential to be adopted as both intake and exhaust valves, which could be manufactured at a maximum cost of 300 yen (JPY) per valve.

6.2 Extremely Low-cost Manufacturing Process

Figure 23 shows the final valve manufacturing process. For the raw material titanium powder, a cheap hydrogenated titanium powder was selected. For the alloying additive, an Al-25Sn-25Zr-6Nb-6Mo-1.2Si (mass%) master alloy powder was developed with the aim of achieving the ultra-high heat resistance required by exhaust valves. In addition, TiB₂ powder was selected as the source of boron for forming the TiB particles. The manufacturing process was as follows: division of each powder into the predetermined weight

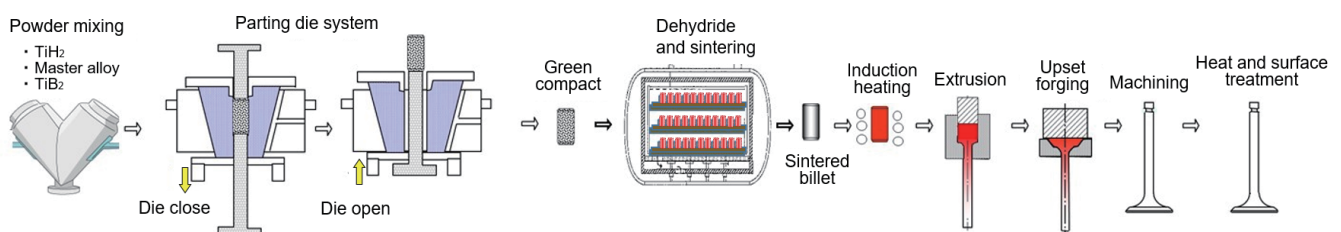


Fig. 23 The developed low-cost engine valve manufacturing process for the TiB particle reinforced B/E Ti-MMC.

proportions \Rightarrow stirring and mixing \Rightarrow compaction into cylindrical billets (dia. 16×42 mm) in a parting die system \Rightarrow heating and dehydrogenation in a vacuum furnace \Rightarrow densification to a relative density of at least 95% at 1300°C \Rightarrow high-frequency induction heating of the sintered billets in air to 1250°C \Rightarrow extrusion of the stem portion of the valves in a ceramic (SIALON: invented 50 years ago at Toyota CRDL⁽²⁷⁾) die \Rightarrow forging into the final valve shape \Rightarrow annealing \Rightarrow machining into the final product shape \Rightarrow oxidation treatment of the seat contact surface and stem by heating in air at approximately 900°C \Rightarrow correction of curvature \Rightarrow inspection \Rightarrow final product.

Adoption of this developed powder metallurgy process enabled the commercialization of titanium valves at much lower cost than conventional titanium valves. A cost of 280 yen (JPY) per valve was achieved, which is in line with the original target and similar to the cost of heat-resistant steel exhaust valves. These cost savings can be summarized into the following four points: (1) the adoption of low-cost hydrogenated titanium powder, (2) the continuous powder mixing \Rightarrow compaction \Rightarrow dehydrogenation \Rightarrow sintering process, which achieved a material yield of roughly 100% and enabled the manufacture of extrudable forging billets, (3) the dispersion of TiB particles, which enabled ultra-high-temperature forging so that the valves could be extruded into the final form, and (4) the formation of wear resistance due to the adoption of an extremely productive and low-cost oxidation treatment in air.

6.3 Selection of Alloy Composition and Optimization of Heat Treatment Conditions

The excellent material properties of the developed Ti-MMC are the result of the synergistic effect between an ultra-heat-resistant matrix and the reinforcement compound particles (TiB). The basic composition of the matrix is determined by the Ti-6Al-4Sn-4Zr-1Nb-1Mo-0.2S (mass%) alloy, which was selected to achieve high-temperature fatigue and creep properties, supplemented by 5 vol% of TiB particles, which was selected to achieve high-temperature strength as well as important properties for component manufacturing, such as ductility, hot workability, machinability, and cost.

The material properties of titanium alloy are closely dependent on its microstructure. In particular, the microstructure of the matrix has a major impact on

high-temperature creep resistance and high-temperature fatigue properties. Specifically, titanium alloys with a coarse acicular microstructure have excellent creep resistances, and titanium alloys with a fine acicular or equiaxed structure have excellent fatigue properties. Therefore, in the case of a normal heat-resistant titanium alloy microstructure, the heat treatment (i.e., the solution treatment and aging) conditions are carefully adjusted to ensure the optimum balance between creep and fatigue properties.

In the case of the developed material, the dispersed TiB particles maximized the β grain growth suppression effect, thereby enabling annealing in the single β phase temperature region, which is difficult to accomplish with ordinary titanium alloys due to the rapid grain coarsening effect in this temperature region. Dispersing the TiB particles also enabled the elimination of the unproductive aging process that tends to drive up costs.

6.4 Effect of TiB Particle Quantity on Mechanical Properties and Hot Workability

Figure 24 summarizes the effects of the TiB particles on material properties at room temperature and elevated temperature of 800 or 850°C . Higher quantities of TiB increase strength and fatigue strength at both room and high temperatures. High-temperature (850°C) fatigue strength is an extremely important property of exhaust valves. TiB particles have a significant effect on this property and a blending amount of around 5 vol% of TiB is sufficient to outstrip the fatigue strength of valve steel (21-4N).

In contrast, dispersion of TiB particles has a slight negative effect on high-temperature creep resistance. This is mainly because the acicular α phase in the matrix becomes finer and adopts an equiaxed structure as the TiB particle content increases. However, the effect of the TiB content is only minor, and superior creep resistance to 21-4N steel can be maintained even at a blending ratio of 10 vol% of TiB.

Room temperature ductility remains virtually constant regardless of the TiB particle content and high-temperature ductility is substantially improved by adding a low amount of TiB particles. Specifically, 5 vol% of TiB has the effect of improving ductility the maximum elongation of approximately 12%. In addition, even 10 vol% of TiB containing alloy maintains ductility by approximately 10%.

Next, this section describes the effects of TiB particles

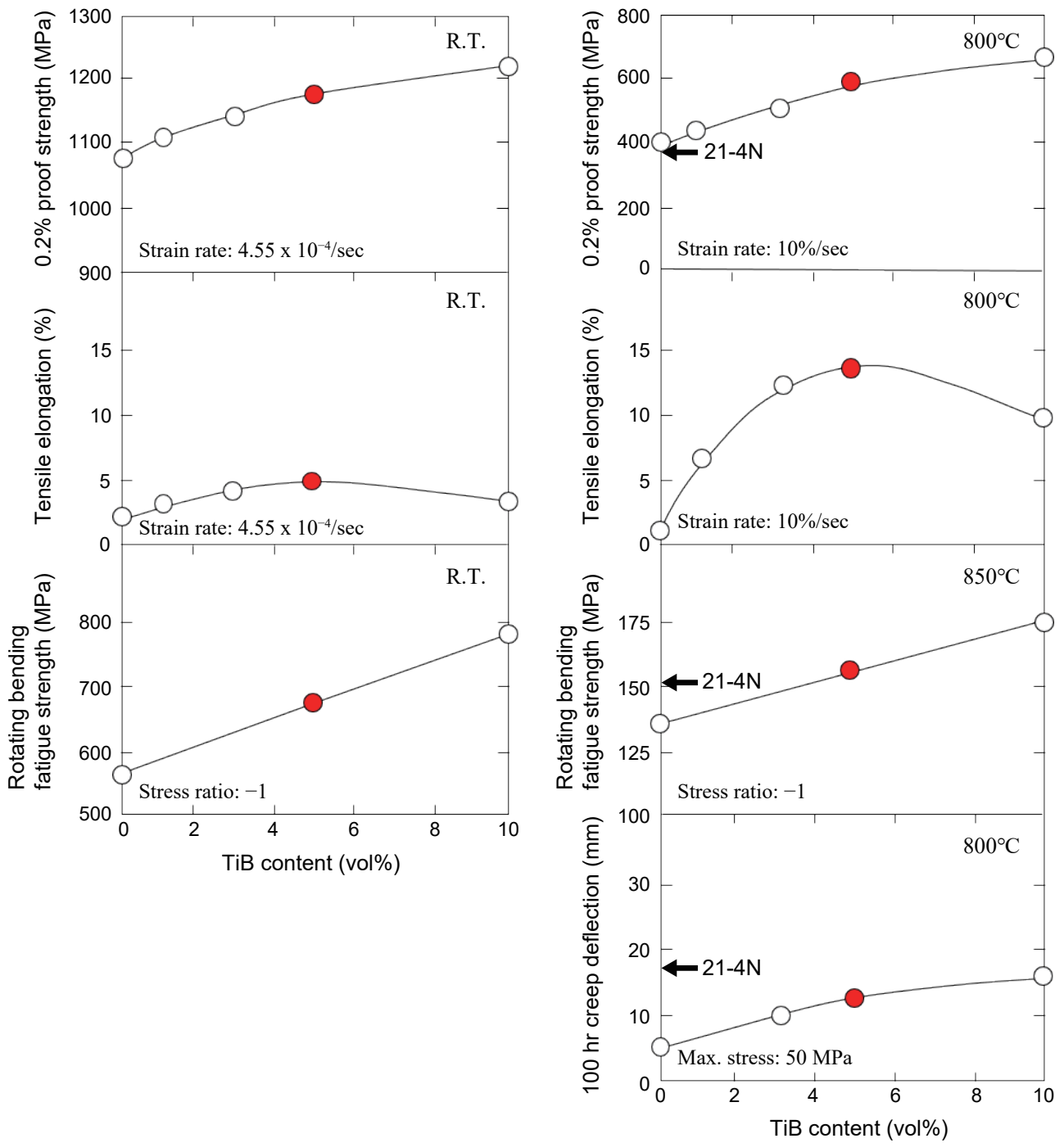


Fig. 24 Changes in mechanical properties of the developed Ti-MMC in accordance with TiB particle content at room and elevated temperatures.

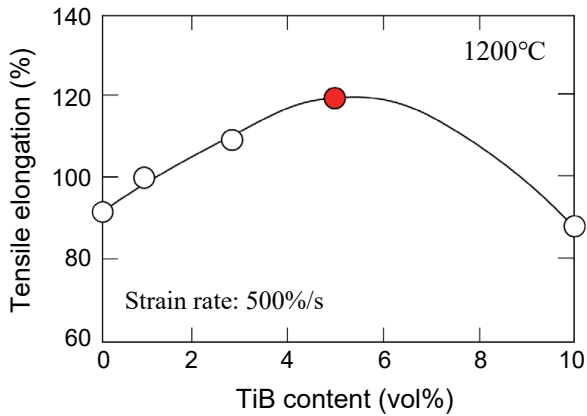


Fig. 25 Effect of TiB particle content on high-temperature ductility at a rapid strain rate.

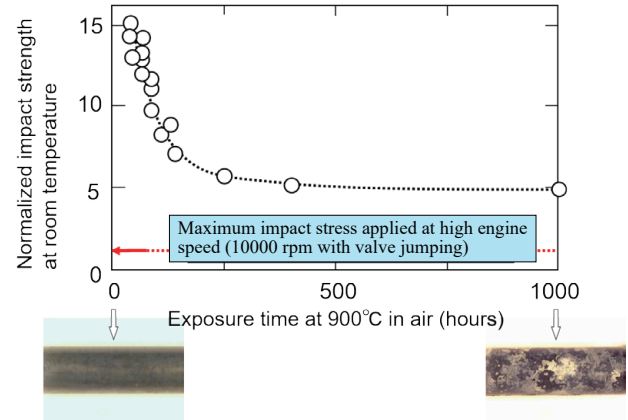


Fig. 26 Example of reliability test results for the developed exhaust valve (impact strength after long term exposure to air at high temperature).

on rapid hot deformability in the actual valve forging temperature region (between 1200 and 1250°C). **Figure 25** shows the relationship between ductility and TiB content when the material is rapidly deformed (500%/s) in the valve forging temperature region. The high-speed ductility at high temperature is virtually consistent with the trend for low-speed (1%/s) elongation at 800°C shown in Fig. 24, which demonstrates that an appropriate TiB particle content has the potential to substantially improve hot workability. This is because the blending of TiB particle suppresses β grain growth during heating, thereby extending the hot working window toward higher temperatures at which working is easier.

6.5 Durability and Reliability of Ti-MMC Exhaust Valves

The previous sections described the development of an MMC with high-temperature strength properties equivalent or superior to the conventional valve steel of the time. However, it was also crucial to ensure wear resistance, which is a vital characteristic for valves. Conventional titanium valves required extremely high-cost surface treatments such as molybdenum spray coating or chromium nitride (CrN) coating. In contrast, this research developed a high-temperature oxidation treatment in air as an effective low-cost alternative. The purpose of oxidation treatment is to improve wear resistance by forming a solid solution with an appropriate quantity of oxygen in the titanium alloy matrix close to the

surface. Combining the dispersion of TiB particles with oxidation treatment in air enabled the development of valve seat contact surfaces with high-temperature wear resistance, valve stems with sliding and wear resistance, and seizure-resistant valve heads.

Next, since titanium alloys have lower oxidation resistance than heat-resistant steel, the research team was concerned about oxidation when used for extended periods in high-temperature combustion gas. The primary reliability requirement of engine valves is that fractures must not occur under any circumstances. As described above, when used under high temperatures, the excellent strength and ductility of this material meant that absolutely no issues occurred in an ultra-high-speed durability test (up to 9500 rpm) designed to generate valve jumping. The issue was reliability under strong impact stress at close to room temperature. An index was created to gauge the reliability of the material impact resistance at room temperature. **Figure 26** shows the results of an impact test conducted at room temperature after exposure to air at 900°C for 1000 hours, assuming the generation of high-temperature oxidation due to usage in a severe driving environment. Although the impact strength decreased substantially due to long-term exposure to high-temperature oxidation in air, the room temperature impact strength of the valve was approximately five times the maximum impact stress likely to cause abnormal valve behavior such as juddering. Consequently, the developed Ti-MMC exhaust valve was verified to be sufficiently reliable for actual usage environments.

6.6 Performance of Ti-MMC as Engine Valves

Although the maximum speed of the new engine installed with the newly developed sintered titanium valves was substantially lowered from 9000 to 7700 rpm for various reasons, this was still 500 rpm higher than the engine it replaced. The developed engine generated a maximum of 210 hp, the highest of any 2000 cc NA engine at the time. The weight of the valve and valve springs was reduced by 40% and 16%, respectively. This lowered high engine speed noise by 30% and camshaft rotational torque by 20%, thereby helping to boost the performance and fuel economy of the engine. In comparison, however, the Honda S-2000 that was launched the following year achieved a maximum engine speed of 9000 rpm and generated 250 hp with heat-resistant steel valves due to the adoption of an ultra-short stroke 2000 cc NA engine incorporating its VTEC technology.

7. Application of Developed Ti-MMC Valves to Toyota Formula 1 Engine^(10,28,29)

Racing car engines operate at extremely high rotational speeds, and reducing the weight of reciprocating parts remains an important requirement to the present day. Since racing cars tend to have lower cost restraints than ordinary vehicles, titanium alloy had already been widely adopted in racing engines. The developed Ti-MMC components were designed to be manufactured at substantially lower cost than conventional titanium alloy components for adoption on mass-produced cars. However, the true potential of this material could not be fully realized in a mass-produced engine. It was thought that more innovative designs that made greater use of the excellent specific strength, specific stiffness, and heat resistance of this material would enable even greater component weight reduction, performance gains, and fuel economy.

In 1999, the year after the launch of the mass-produced Altezza installed with these titanium-based valves, Toyota announced its decision to participate in F1 and started up a constructor team (Panasonic Toyota Racing) to develop both a racing engine and chassis under the auspices of Toyota Motorsport GmbH (TMG) located in the outskirts of Cologne, Germany. Even after the International Automobile Federation (FIA) changed the regulated engine from a V10 to

a V8 configuration, further weight reduction in the valve train was required to realize engine speeds in excess of 20000 rpm. Dr. Luca Marmorini, the Technical Director of TMG's F1 engine division, noticed the new material (Ti-MMC) developed for mass-produced vehicles by Toyota CRDL. At that time, the engines of every F1 team, including Toyota, used titanium valves supplied by the U.S. company Del West Engineering, Inc. It was judged that the Toyota original material (Ti-MMC) had a higher potential than the titanium alloy manufactured by Titanium Metals Corporation (TIMET) and used by Del West in terms of strength, stiffness, and heat resistance. Therefore, the new material was seen as having a higher potential ceiling for improving valve performance.

Since the cooling performance of the cylinder head in an F1 engine is far superior to the cylinder heads in mass-produced cars, the temperature rise of the exhaust valves can be minimized. As a result, the developed exhaust valve material, which was primarily aimed for mass-produced cars, was found to be perfectly adequate for the exhaust valves of an F1 engine. In contrast, since the intake port of an F1 engine is much hotter than in a mass-produced vehicle, the intake valves are exposed to comparatively higher temperatures. For this reason, the heat resistance of the Ti-6Al-4V alloy used for the mass-produced intake valves was insufficient. In addition, F1 engine intake valves are designed with a larger head diameter and smaller stem diameter for greater intake efficiency. Consequently, the intake valve material for an F1 engine must have higher strength and creep properties than a mass-produced material. Therefore, the composition of the intake valve matrix alloy was changed to the same Ti-6Al-4Sn-4Zr-1Mo-1Nb-0.2Si (mass%)-based near- α alloy composition with high heat resistance that was used to develop the exhaust valves. The TiB particle content was also doubled (10 vol%) compared to the MMC developed for the exhaust valves. **Figure 27** compares the appearance of the Ti-MMC intake valves used on the mass-produced Altezza and in the F1 engine. There are clear differences in head and stem diameters.

Figure 28 compares the relative mechanical properties of the new MMC developed for the F1 engine intake valves with those of the previous Ti-6Al-4V alloy used in the Altezza. The figure shows that the F1 material has far greater strength, stiffness, and heat resistance. Increasing fatigue strength and creep

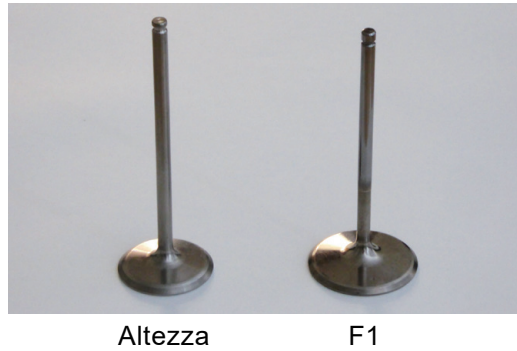


Fig. 27 Different appearances of the intake valves for the mass-produced 3S-GE engine (left) and RVX-09 racing engine (right).

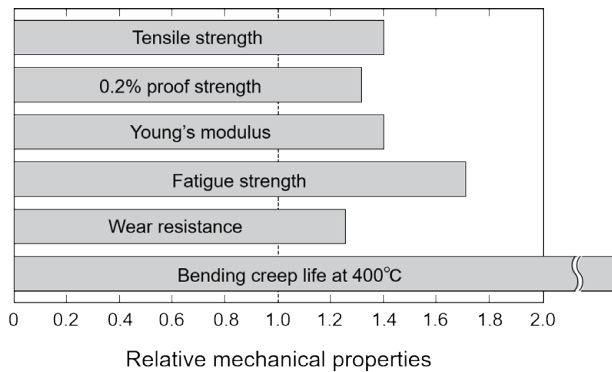


Fig. 28 Comparison of the mechanical properties of the developed MMC for F1 intake valves relative to those of the Altezza intake valve.

properties are particularly important ways of creating a greater margin in terms of component durability. In addition to reducing weight and enabling designs with higher efficient intake geometry, this approach also helped respond to increasingly stringent regulations. Specifically, in 2006, when the regulated V10 engine was changed to a V8 configuration, the minimum permitted engine life was only two races (a total driving distance of around 500 km). In 2009, teams were prohibited from changing engines for eight races (at least 2200 km), tough conditions that were difficult for every team to satisfy. The Ti-MMC valves developed all inside Toyota Group companies (including original material and manufacturing process) were recognized as making a major contribution to Toyota's substantial improvement in engine power under these conditions.

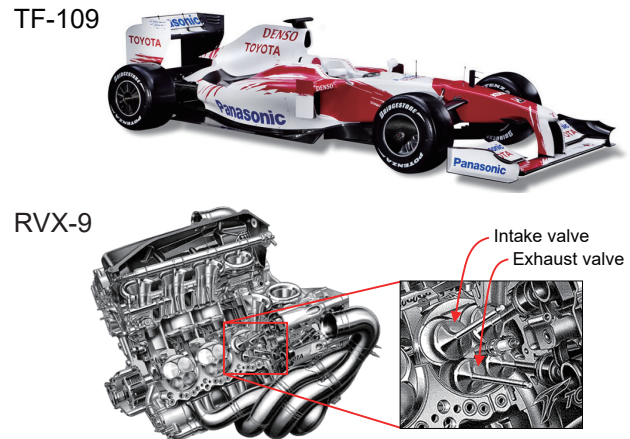


Fig. 29 Appearance of Panasonic-Toyota Racing F1 car (TF-109) and cutaway view of 2398 cc NA V8 engine (RVX-09).

The engine installed with the developed Ti-MMC valves was adopted in 2007. The performance of the engine was superior to that of other teams. In 2009, immediately before Toyota decided to withdraw from F1, this engine helped Toyota to achieve one pole position, two fastest laps, and five podium finishes (**Fig. 29**). Unfortunately, Toyota was unable to achieve its aim of standing on the center of the podium.

8. Achieving Further Cost Reductions

8.1 Issues of Mass-produced Ti-MMC Engine Components

The manufacturing cost of the developed Ti-MMC valves satisfied the original targets and helped to realize a unit price of less than 300 yen (JPY) per valve. In conclusion, although the initial objective of adopting titanium alloy in a mass-produced car was achieved, titanium alloy has unfortunately yet to establish itself as a multi-purpose automotive material. Titanium is a feasible alternative for engine valves made from high-cost heat-resistant steel, but further cost reductions will be necessary before titanium alloy can be adopted in a wider selection of parts requiring specific strength and specific stiffness.

The previous sections have described a comparatively straightforward engine valve manufacturing process in which a simple cylindrical billet is extruded and forged at ultra-high temperatures of 1200°C or higher,

something that had not previously been thought possible for titanium. This is a special case where high-yield net shaping is feasible. However, general mechanical components often have complex shapes that require the application of multiple machining processes (Fig. 4) to a forging to achieve net shaping, which results in a substantial reduction in yield. In contrast, the B/E method enables the raw material powder to be compacted into a net shape in a die. Converting this into the finished component by sintering alone would enable massive cost savings. This approach is identical to the current manufacturing process for sintered steel components, and to realize it with titanium, the following minimum conditions had to be satisfied.

- (1) The sintered part must satisfy requirements for mechanical properties and reliability without further processing such as heat treatment.
- (2) The sintered part must have sufficient dimensional accuracy for it to function properly without further machining.
- (3) Mass-production using a continuous sintering furnace must be possible.

The developed process is capable of achieving high densities in excess of 97% after sintering and reducing the size of the pores in the material. However, further densification would be preferable to ensure sufficient reliability.

8.2 Development of Ultra-high-density Compaction Technology⁽³⁰⁾

The fastest way to increase the density of the sintered material to as close as possible to the true density is to raise the density of the green compact. However, the compacting pressure cannot simply be raised indiscriminately. Since titanium is susceptible to adhesion to the die, high pressure compaction is likely to result in a phenomenon known as die galling. Ordinarily, small amounts of lubricant are mixed with the powder to prevent seizure. However, increasing the lubricant content has an adverse effect on the properties of the product since the heating process to eliminate the wax lubricant causes reactions with the titanium and generates impurities in the material. Therefore, the lubricant content must be minimized and it is difficult to increase the compacting pressure above 600 MPa. In response to these issues, innovative die lubrication technology was developed that enabled ultra-high-density powder molding with

compacting pressures up to 2000 MPa. An outline of these technologies is described below.

The key aspect of this technology is the combination of lithium stearate (Li-Ste.) as a die lubricant with warm compaction at around 150°C. This approach was discovered by chance in the second half of the 1990s by a visiting student researcher from Fraunhofer IFAM Germany, who was working at Toyota CRDL to identify lubricants for powder forming dies. Although the initial research was focused on ferrous powders die lubrication methods, it was discovered that applying this approach with titanium powder achieved a far greater lubrication effect than with ferrous powders. **Figure 30** shows an outline of the developed compaction method. In this method, an aqueous solution containing 1 mass% of Li-Ste. is sprayed into a die warmed to approximately 150°C, forming an Li-Ste. film on the walls of the die. The die is then filled with raw material powder and compacted. **Figure 31** compares the relationship between the die ejection force after compaction with the compacting pressure for a coarse titanium powder (HDH: -#150). The compacting conditions are (a) compacted at room temperature lubricated with the conventional zinc stearate (Zn-Ste.) and (b) compacted at 150°C lubricated with Li-Ste., respectively. With the conventional compaction method, the ejection force continues to increase in accordance with the compacting pressure. In contrast, with the developed warm compaction method, the increase in ejection force tops out at around a compacting pressure of 600 MPa before decreasing as the compacting pressure increases. The ejection force then stabilizes at around 1000 MPa and remains extremely low (approximately 5 MPa) even at a compacting pressure of 1960 MPa. Although the data for ferrous powders is almost identical to the

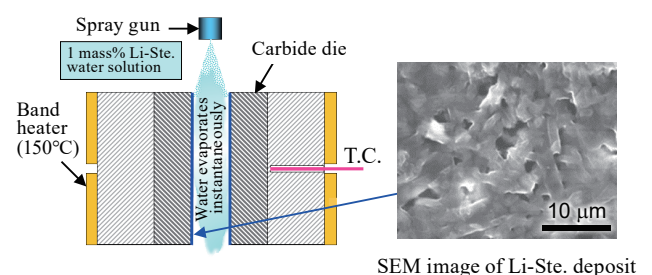


Fig. 30 Configuration of the metallic mold for the ultra-high-pressure warm compaction.

results shown in Fig. 31, the amount of spring back with titanium is close to three times that of steel, which means that the lubricating effect of the Li-Ste. is stronger with titanium powder than the steel powder. **Figure 32** shows the results of the same experiment conducted with a fine titanium powder (HDH: -#350). The ejection force after compaction did not exceed 1 MPa at almost all compacting pressures up to 1960 MPa. In summary, the developed method is capable of extracting particle compacts compressed at ultra-high pressures from the die using an ejection

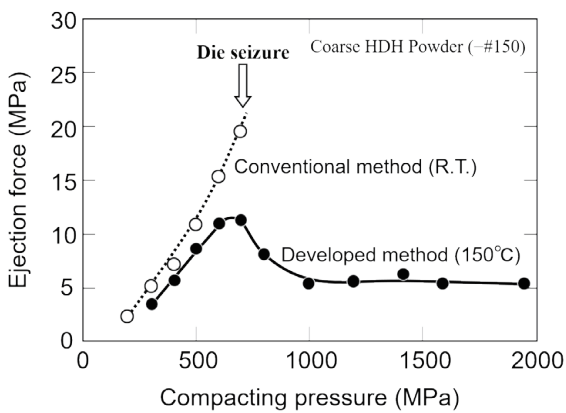


Fig. 31 Relationship between ejection force and compacting pressure for conventional compaction and the developed warm compaction using a coarse HDH titanium powder (TS-150).

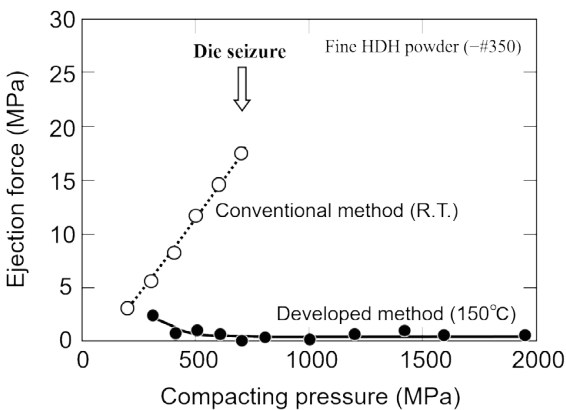


Fig. 32 Relationship between ejection force and compacting pressure for conventional compaction and the developed warm compaction using a fine HDH titanium powder (TS-459).

pressure of only several kg/cm². Considering the huge elastic stress generated by spring back in the compacted titanium powder, this is regarded as a super-lubrication phenomenon with a frictional force of virtually zero.

Figure 33 compares the appearance of die sliding surfaces of pure titanium powder compacts. The compact on the left was molded normally at a compacting pressure of 686 MPa. The compact on the right was molded by the developed method at a compacting pressure of 1960 MPa. The conventional green compact (pressure: 686 MPa) shows clear evidence of titanium adhesion (die galling), indicating that the compacting pressure limit was exceeded. In contrast, the surface of the 1960 MPa particle compact is glossy and shows absolutely no evidence of adhesion.

Figure 34 illustrates the likely mechanism of this super-lubrication phenomenon. Time of flight-secondary ion mass spectroscopy (TOF-SIMS) was carried out

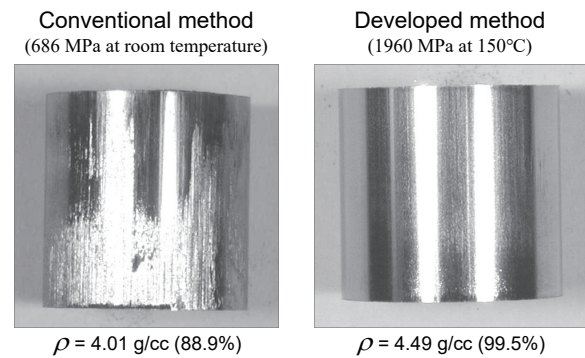


Fig. 33 Appearance of pure titanium green compacts (HDH: TS-150).

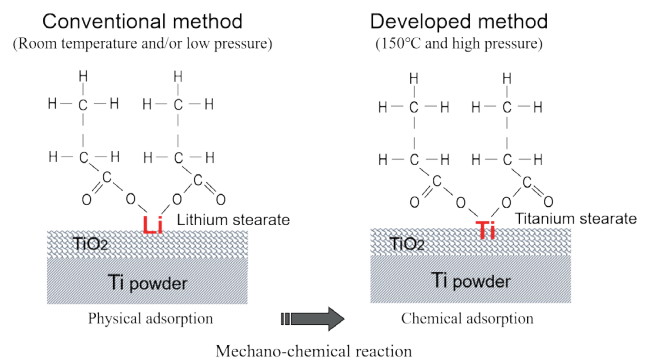


Fig. 34 Outline of lubricating film transformation on the surface of titanium particles during high pressure warm compaction (TOF-SIMS).

on the side wall surface of the particle compacts. Analysis results showed that the Lt-Ste. die coating adhered to the surface of the room temperature particle compact without transformation. In contrast, the Li-Ste. transformed into a titanium stearate (Ti-Ste.) at the surface of the warm compaction/high-pressure compact. Specifically, the interaction of the appropriate temperature (150°C) and high pressure (higher than 600 MPa) causes a mechano-chemical reaction between the Li-Ste. coated on the die wall and the titanium powder surface, transforming the Lt-Ste. into Ti-Ste. This Ti-Ste. is strongly chemically adsorbed by the surface of the titanium powder (i.e., the particle compact), and the super-lubrication phenomenon described above appears between the Li-Ste., which is physically adsorbed by the surface of the die.

Figure 35 shows the relationship between relative density and compacting pressure in the case of a Ti-6Al-4V alloy green compact molded using the developed method, and the same particle compact after sintering at 1300°C for four hours. The relative density of the sintered compact increases in accordance with the compacting pressure, rising from around 96% at 490 MPa to over 99% at compacting pressures at and above 1000 MPa. Although achieving a sintered compact with close to the true density will naturally help to improve reliability, the important point of these results is the density gap between the green compact and sintered compact decreases as the compacting pressure increases. **Figure 36** shows the relationship between dimensional change after sintering and compacting pressure. At normal compacting pressures (under 500 MPa), sintering causes dimensional shrinkage of more than 3%. In contrast, with the developed method, dimensional change decreases as the compacting pressure rises, falling to an extremely low level of less than 1% at pressures over 1000 MPa. This means that post-sintering machining can be minimized by increasing the compacting pressure to as high a value as possible. Although reducing the requirement for post-sintering machining helps to greatly lower costs, the ideal situation is to eliminate machining entirely and use the sintered skin without further processing. However, the fatigue strength and other properties of the sintered skin must be sufficient to allow the sintered skin to be used. **Figure 37** shows the results of a four-point bending fatigue test using thin-plate sintered components (Ti-6Al-4V alloy), with the top and bottom surfaces used as the die press

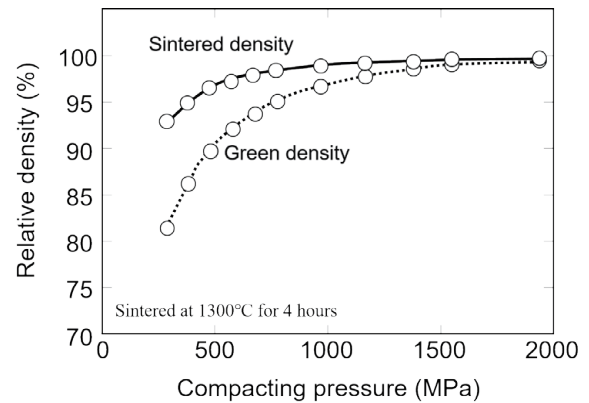


Fig. 35 Relationship of green and sintered densities with compacting pressure for the developed warm compaction using a coarse HDH titanium powder (TS-150).

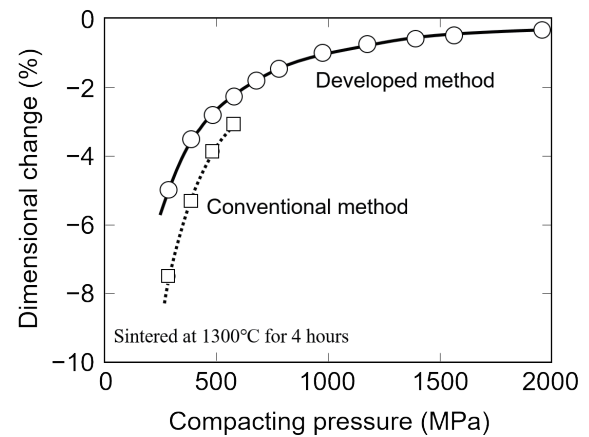


Fig. 36 Relationship between dimensional change after sintering and compacting pressure for the developed warm compaction using a coarse HDH titanium powder (TS-150).

surfaces. The graph compares the results of sintered skins compacted conventionally at a pressure of 392 MPa and the developed method at a pressure of 1568 MPa. A clear difference between the conventional and high-density compacts can be seen at 10^5 cycles. At 10^7 cycles, the durability of the high-density compact is five times higher than the conventional compact. This graph also compares the high-density compact sintered skin with an ingot metallurgy forged plate after machining. Virtually almost the same results were achieved at all cycles, which demonstrates that a high-density compact sintered skin has comparable fatigue properties to a machined I/M forge product.

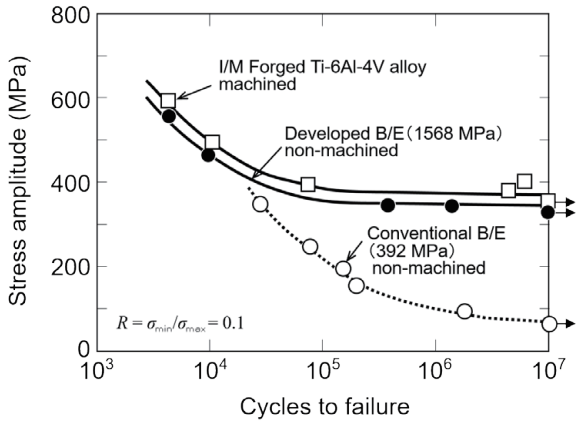


Fig. 37 Comparison of four-point bending fatigue property of as-sintered Ti-6Al-4V alloy via different method carried out on non-machined surface.

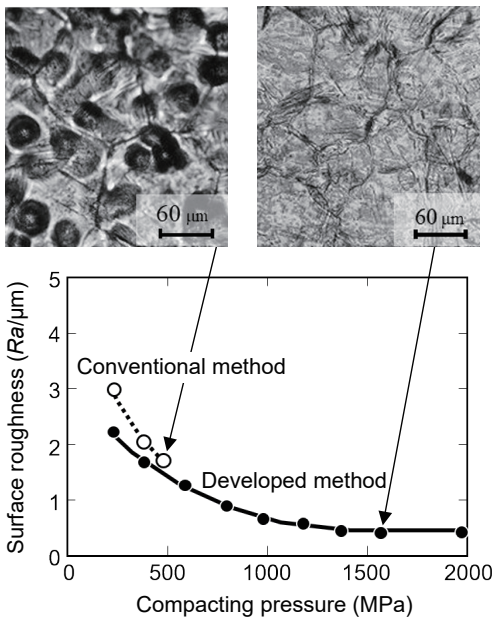


Fig. 38 Comparison of the surface roughness and morphology of sintered compacts manufactured using the conventional and developed compacting methods.

Figure 38 compares the surface of sintered compacts manufactured at 392 and 1562 MPa. Compared to the surface roughness of the conventional compact ($Ra =$ approximately $3.0 \mu\text{m}$), the surface roughness of the high-pressure compact was only $Ra = 0.5 \mu\text{m}$ or less, which is almost equivalent smoothness to that of a machined part.

8.3 Improving Productivity Using Continuous Sintering Furnace^(31,32)

The research described in the previous section demonstrated that a sintered skin manufactured by the B/E method has equivalent mechanical properties to a high-cost ingot forged and machined part. However, the sintering is carried out in a vacuum furnace, which is a batch process with low-productivity and a major obstacle to reducing cost. Adopting the same type of belt-type continuous sintering furnace as conventional sintered steel parts might enable further substantial cost reductions. In the second half of the 1990s, this research focused on the ultra-low-oxygen partial-pressure continuous-furnace⁽³³⁾ developed by Kanto Yakin Kogyo Co., Ltd. under the name “Oxynon”. In summary, this is a belt furnace with an inert gas atmosphere. Critically, the interior of the furnace is completely manufactured from carbon, including the heater, mesh belt and muffle. By including a small amount of oxygen ($< 10^{-3}$ atm) in the inert gas atmosphere, this oxygen reacts with the carbon in the furnace to maintain the Boudoir equilibrium, which can be expressed as $2C + O_2 \Rightarrow 2CO$. As a result, the inside of the furnace maintains an incredibly low oxygen partial pressure of between 10^{-20} and 10^{-27} atm, which forms deoxygenation conditions for titanium at sintering temperatures between 1200 and 1300°C. **Figure 39** shows an outline of the Oxynon furnace configuration. **Figure 40** compares the tensile properties of a Ti-6Al-4V sintered alloy manufactured in a vacuum furnace ($< 10^{-5}$ torr) and the Oxynon continuous furnace (in an argon atmosphere). There is virtually no difference in mechanical properties at any sintering temperature. This research demonstrated that titanium parts can be sintered to the same quality in a mass-production continuous belt furnace as in a vacuum furnace of batch operations.

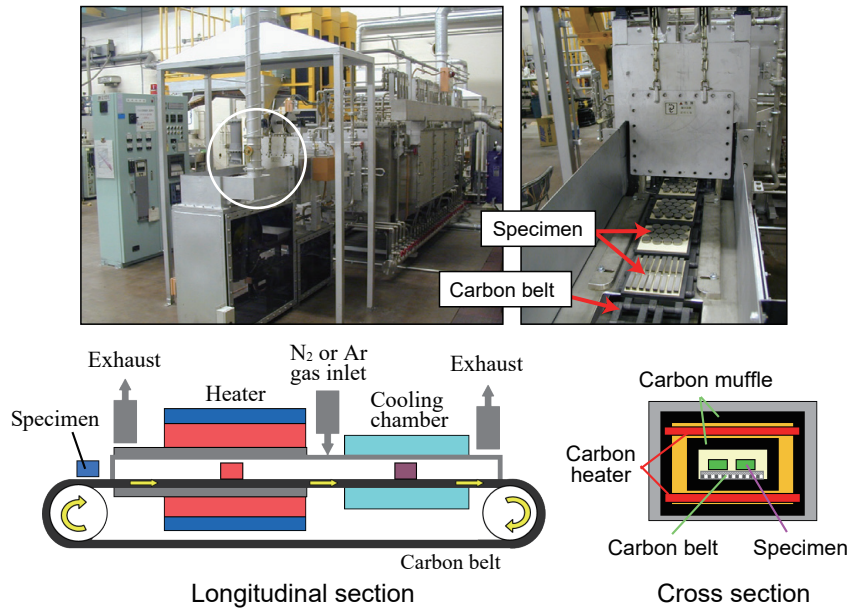


Fig. 39 Configuration of the ultra-low oxygen partial pressure continuous furnace (Oxyton).

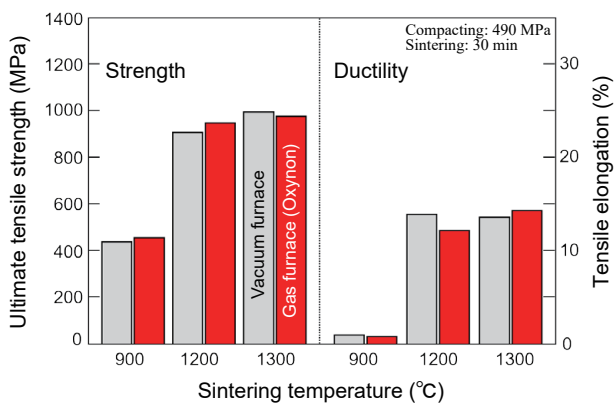


Fig. 40 Comparison of tensile properties of B/E Ti-6Al-4V alloy with different types of sintering furnace.

9. Proposal for the General Adoption of Titanium (in Place of a Conclusion)

To cast aside the preconceived idea that titanium is too high-cost for application to mass-produced automotive parts, Toyota CRDL worked for about fifteen years from the middle of the 1980s to the beginning of the 2000s to drastically reduce the cost and substantially improve the performance of titanium components. These efforts successfully resulted in materials far

superior to conventional titanium alloys in terms of cost and performances (**Fig. 41**). In addition to lower cost, in 1998, Toyota CRDL helped to develop a mass-produced engine exhaust valves, something that was thought to be impossible in terms of performance. Even higher performance valves were then adopted by the F1 engine used by Panasonic Toyota Racing from 2007.

Through the development of ultra-high-density powder compaction and continuous sintering technologies, which was carried out alongside the practical adoption of the titanium-based engine valves, major progress was made toward further lowering the manufacturing cost of titanium components to a level far beyond the conventional conception of titanium alloy. However, the original goal of this research, which was to achieve manufacturing costs equivalent to steel components has yet to be achieved. The price of raw material titanium powder is too high to consider titanium as a multi-purpose automotive material. Machining costs were also minimized by achieving a material yield of almost 100% through extreme densification and dimensional accuracy. The application of continuous sintering also helped to realize drastic improvements in productivity. The final cost of manufacturing a titanium component is the total of the raw material powder cost and the process running costs (powder mixing

⇒ compacting ⇒ sintering). These running costs decrease as the production volume increases, bringing the product price close to the price of the raw material powder. When research into sintered titanium began in the 1980s, it was possible to obtain extremely low-cost (lower than U.S. \$10/kg) and high-performance HSF titanium powder manufactured by the Hunter method. However, in the first half of the 1990s, titanium smelting technology using the Hunter method was expelled on a global scale by the Kroll method. As a result, from the 1990s, it was only possible to obtain high-cost (higher than U.S. \$20/kg) HDH powder manufactured from sponge titanium by the Kroll method. By chance, the low-cost hydrogenated titanium powder used to manufacture these valves was particularly suited to the green compact ⇒ dehydrogenation ⇒ vacuum sintering ⇒ hot extrusion forging manufacturing process. However, this powder is not particularly suited to the innovative combination of ultra-high-density powder compaction and sintering in an inert gas continuous furnace. If the price of pure titanium powder falls comparable to that of the Hunter sponge fine (around U.S. \$10/kg), it is not beyond the realms of possibility that high-performance sintered Ti-MMC can be adopted for a wide range of automotive components beyond valves. It is hoped that low-cost pure titanium powder equivalent to HSF will once again appear on the market.

In the first half of the 1980s, Toyota launched the world's first powder forged steel connecting rod.⁽³⁴⁾ Since then, sinter forging technology has become widely used by automakers around the world and is now firmly established as a high-quality low-cost process with extremely high product weight accuracy compared with conventional ingot forging method. It is thought that sinter forging can be adopted as-is to the manufacture of Ti-MMC components. Specifically, this would entail sintering a near net-shaped sintered preform in an Oxynon continuous furnace, transporting it to the press while maintaining the sintered compact at the sintering temperature, and then directly forming the product by hot forging. This approach has major potential as a low-cost manufacturing process for ultra-high-performance Ti-MMC products.

Finally, this article concludes by introducing an example application that combines sintering and hot working. **Figure 42** shows several prototype engine parts made of the TiB/Ti-MMCs. In addition to the commercialized engine valves, feasibility studies were conducted on spur gears, connecting rods, valve lifters, valve retainers, hollow valves, and so on. The spur gear shown in Fig. 42 was manufactured from 20 vol% TiB/Ti-7Mo-4.5Fe-1.5Al-1.5V MMC by applying a high frequency induction heating to the circumference of a disk-shaped ring sintered compact in air and then carrying out roll-forming. Although it is very important

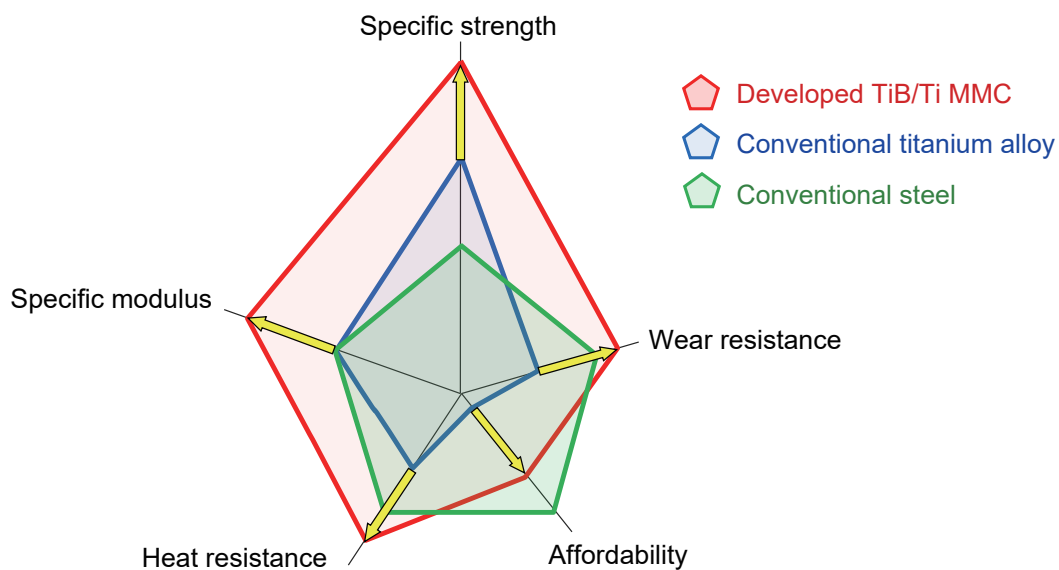


Fig. 41 Radar chart comparing typical properties of the developed TiB/Ti-MMC, conventional titanium alloy, and conventional steel.

to reduce the weight of gears, the extremely high stress applied to the gear teeth means that both high stiffness and rolling wear fatigue properties of the material are equally important. For this reason, there have been no proposals to use materials other than steel for these parts. However, with a high TiB content, the developed Ti-MMC can achieve the mechanical properties equivalent to gear steels with high fatigue strength and rolling wear resistance, at substantially lower weight (less than 60% of steel). In addition, by optimizing the matrix alloy composition, it may be possible to realize

a sintered compact with a high density of at least 98% of the true density even if the TiB particle content increases up to 40 vol% (Figs. 43 and 44).⁽³⁵⁾ This extreme densification phenomenon at high volume of TiB particles was verified to be achieved via a unique activated sintering mechanism brought by coexistence of B, Fe, and Mo.⁽³⁵⁾ In addition, since this MMC also has excellent hot workability,⁽²⁵⁾ it can be easily hot roll-formed into the gear shape shown in Fig. 42. This prototype gear is an indication of the future wider potential of titanium.



Fig. 42 Prototype automotive parts made of TiB/Ti-MMC produced by the developed B/E process: spur gear, connecting rod, valve lifter, valve retainer, and hollow valve, etc.

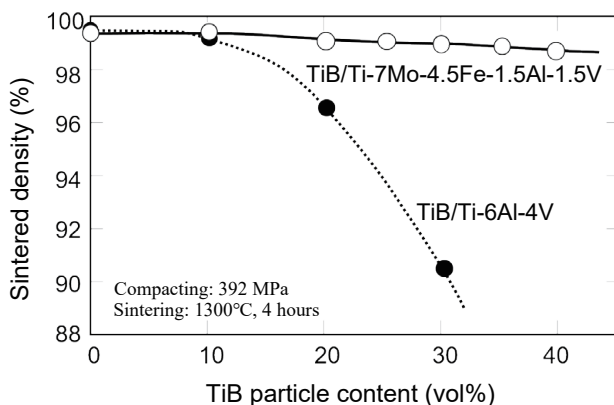


Fig. 43 Relationship of sintered density of Ti-7Mo-4.5Fe-1.5Al-1.5V based and Ti-6Al-4V based MMCs with TiB particle content obtained by the developed B/E process.

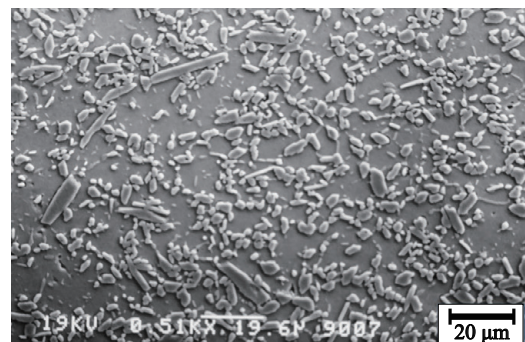


Fig. 44 Sintered microstructure of 30 vol% TiB/Ti-7Mo-4.5Fe-1.5Al-1.5V MMC compacted at 392 MPa followed by sintering at 1300°C for 4 hours ($\rho/\rho_0 = 99\%$).

References

- (1) Furuta, T. and Saito, T., "Titanium Alloy Matrix Micro Composite by Reaction Sintering", *Current Advances in Materials and Processes* (in Japanese), Vol. 4, No. 5 (1991), p. 1740.
- (2) Saito, T., Furuta, T., Yamaguchi, T. and Ogino, K., "A New Low-cost MMC of TiB Particle Dispersed in Titanium Alloy", *Proc. Powder Metall. World Congr.* (1993), pp. 642-645, JSPM.
- (3) Saito, T. and Furuta, T., "Development of High Performance Titanium Matrix Composite", *R&D Rev. Toyota CRDL* (in Japanese), Vol. 29, No. 3 (1994), pp. 49-60.
- (4) Saito, T., Furuta, T. and Yamaguchi, T., "A Low Cost Titanium Alloy Matrix Composites", *Metall. Technol. Pract. Titanium Alloys, Proc. 1st Int. Symp. Metall. Tech. Pract. Titanium Alloys* (1994), pp. 351-362, TMS.
- (5) Saito, T., Furuta, T. and Yamaguchi, T., "Development of Low Cost Titanium Alloy Matrix Composite", *Recent Advances in Titanium Metal Matrix Composites: Proc. Symp. Held during Materials Week* (1995), pp. 33-44, TMS.
- (6) Saito, T., "A Cost-effective P/M Titanium Matrix Composite for Automobile Use", *Advanced Performance Materials*, Vol. 2, No. 2 (1995), pp. 121-144.
- (7) Yamaguchi, T., Morishita, H., Iwase, S., Yamada, S., Furuta, T. and Saito, T., "Development of P/M Titanium Engine Valves", *SAE Tech. Pap. Ser.*, No. 2000-01-0905 (2000).
- (8) Furuta, T., Saito, T. and Yamaguchi, T., "Development of Titanium Metal Matrix Composite Exhaust Valve", *R&D Rev. Toyota CRDL* (in Japanese), Vol. 36, No. 1 (2001), pp. 51-56.
- (9) Furuta, T., Yamaguchi, T., Shibata, Y. and Saito, T., "P/M Titanium Metal Matrix Composite for Exhaust Valve", *Titanium '99: Science and Technology: Proc. 9th World Conf. Titanium* (2000), pp. 1917-1924, CRISM.
- (10) Takeuchi, K. and Yajima, H., "Toyota F1 Engine", *Engine Technol. Rev.* (in Japanese), Vol. 2, No. 1 (2010), pp. 14-20.
- (11) Okamoto, T., Nagai, M., Kawamura, H., Tsukamoto, K. and Maruyama, H., "Development of V10 4.8-liter 1LR-GUE Engine for the Lexus LFA", *Toyota Tech. Rev.* (in Japanese), Vol. 57, No. 2 (2011), pp. 67-71.
- (12) Sugawara, J., Suzuki, K., Kinoshita, Y., Tsukamoto, K., Tada, H. and Kawamura, H., "Development of the New 2UR-GSE Engine for the LEXUS Premium Sports RC F", *Yamaha Motor Tech. Rev.* (in Japanese), Vol. 51 (2015), pp. 10-15.
- (13) Saito, T. and Furuta, T., "Microstructure and Sintering Behavior of Ti-6Al-4V Alloy", *Current Advances in Materials and Processes* (in Japanese), Vol. 4, No. 5 (1991), pp. 1738-1739.
- (14) Saito, T. and Furuta, T., "*Shōketsu Chitan Gōkin: Sofun'matsu Kongōhō no Kikaiteki Seishitsu*", *R&D Rev. Toyota CRDL* (in Japanese), Vol. 26, No. 1 (1991), pp. 44-61.
- (15) Saito, T. and Furuta, T., "A New B/E Process for High Strength P/M Titanium Alloy", *Proc. Powder Metall. World Congr.* (1993), pp. 606-609, JSPM.
- (16) Froes, F. H. and Eylon, D., "Powder Metallurgy of Titanium Alloys: A Review", *Titanium: Science and Technology* (1985), pp. 267-286, Deutsche Gesellschaft für Metallkunde.
- (17) Froes, F. H., Eylon, D. and Bomberger, H. B., *Titanium Technology: Present Status and Future Trends* (1985), 191p., Titanium Development Association.
- (18) Roberts, P. R. and Lowenstein, P., "Titanium Alloy Powders Made by the Rotating Electrode Process", *Powder Metallurgy of Titanium Alloys* (1980), pp. 21-35, The Metall. Soc. AIME.
- (19) Kosinski, E. J. "The Mechanical Properties of Titanium PM Parts Produced from Superclean Powders", *Progress in Powder Metallurgy*, Vol. 38 (1982), pp. 491-502, MPIF.
- (20) Kelto, C. A., "Rapid Omnidirectional Compaction", *Metals Handbook*, Vol. 7 (1984), pp. 542-546, ASM.
- (21) Andersen, P. J. and Eloff, P. C., "Development of Higher Performance Blended Elemental Powder Metallurgy Ti Alloys", *Powder Metallurgy of Titanium Alloys* (1980), pp. 175-187, The Metall. Soc. AIME.
- (22) Eylon, D., Vogt, R. G. and Froes, F. H., "Property Improvement of Low Chlorine Titanium Alloy Blended Elemental Powder Compacts by Microstructure Modification", *Progress in Powder Metallurgy*, Vol. 42 (1986), pp. 625-634.
- (23) Graham, D., "A Summary of the Impurity Diffusion to Beta Phase of Titanium", *Diffusion in Body-centered Cubic Metals* (1965), pp. 27-35, American Society for Metals.
- (24) Froes, F. H. and Storer, J., *Recent Advances in Titanium Metal Matrix Composites* (1995), 293p., TMS.
- (25) Saito, T., Takamiya, H. and Furuta, T., "Thermomechanical Properties of P/M β Titanium Metal Matrix Composite", *Material Science and Engineering*, Vol. 243, No. 1-2 (1998), pp. 273-278.
- (26) Saito, T., "The Automotive Application of Discontinuously Reinforced TiB-Ti Composites", *JOM*, Vol. 56, No. 5 (2004), pp. 33-36.
- (27) Oyama, Y. and Kamigaito, O., "Solid Solubility of Some Oxides in Si_3N_4 ", *Jpn. J. Appl. Phys.*, Vol. 10, No. 11 (1971), pp. 1637-1642.
- (28) Suzuki, T., Ikehata, H., Takamiya, H. and Saito, T., "*Ryūshi Kyōka-gata Chitan Gōkin no F1 Enjin e no Tekiyō*", *Proc. 23rd Meet. 123rd Comm. Heat Resisting Materials and Alloys (123 HiMAT)* (in Japanese), Vol. 54, No. 3 (2013), pp. 357-365, JSPS.
- (29) "Toyota RVX-09 (2009)", *Motor Fan Illustrated, Special Edition* (in Japanese) (2010), pp. 16-23.

- (30) Takamiya, H., Kondoh, M. and Saito, T., "Ultra-high Pressure Warm Compaction for P/M Titanium Components", *Cost-affordable Titanium* (2004), pp. 185-192, TMS.
- (31) Saito, T., "Ti-B Alloy for Automobile Use: Remaining Issues", presented at: Titanium Alloys Modified with Boron Workshop; 2005 October 11, Dayton, OH, TMS.
- (32) Saito, T., "New Titanium Products via Powder Metallurgy Process", *Ti-2003, Science and Technology: Proc. Conf. 10th World Conf. Titanium* (2003), pp. 399-410, Wiley-VCH.
- (33) Kanda, K., "Development and Application of the Continuous Atmosphere Controlled Furnace 'OXYNON'", *J. Advanced Science* (in Japanese), Vol. 16, No. 1 (2004), pp. 7-11.
- (34) Ohnishi, T., Takahashi, A., Tsumuki, C. and Nagare, I., "Shōketsu Tanzō Konroddo no Kaihatsu", *Bulletin of the Japan Institute of Metals* (in Japanese), Vol. 22, No. 6 (1983), pp. 537-539.
- (35) Saito, T., Furuta, T. and Takamiya, H., "Sintering Behavior and Thermal Stability of a TiB Particle Reinforced PM Beta-Titanium Matrix Composite", *Titanium '95: Science and Technology: Proc. 8th World Conf. Titanium* (1995), pp. 2763-2770.

Fig. 1 (upper row)

Reprinted from Altezza Qualitat catalog (2000), © 2000 TOYOTA CUSTOMIZING & DEVELOPMENT Co., Ltd., with permission from TOYOTA CUSTOMIZING & DEVELOPMENT Co., Ltd.

Fig. 2 (upper row)

Reprinted from LFA photo gallery (<https://lexus.jp/models/lfa/gallery/>), © 2020 LEXUS.

Fig. 2 (lower row)

Reprinted from Motor Fan Illustrated, Special Edition (2010), pp. 16-23, Toyota RVX-09 (2009), © 2010 SAN-EI CORPORATION, with permission from SAN-EI CORPORATION.

Figs. 5, 10, 13-14 and Tables 1-3

Reprinted from R&D Rev. Toyota CRDL, Vol. 29, No. 3 (1994), Saito, T. and Furuta, T., Development of High Performance Titanium Matrix Composite, © 1994 TOYOTA CRDL., INC.

Figs. 24-25

Reprinted from SAE Tech. Pap. Ser., No. 2000-01-0905 (2000), Yamaguchi, T., Morishita, H., Iwase, S., Yamada, S., Furuta, T. and Saito, T., Development of P/M Titanium Engine Valves, © 2000 SAE International, with permission from SAE International.

Fig. 29 (upper row)

Reprinted from Toyota Gazoo Racing, TOYOTA F1 Archive 2002-2009, TF109 (<https://toyotagazooracing.com/archive/ms/jp/F1archive/team/tf109/index.html>), © 2009 Toyota Motor Corporation with permission from Toyota Motor Corporation.

Fig. 29 (lower row)

Reprinted from Motor-Fan TECH (<https://motor-fan.jp/tech/10012932>), © 2019 SAN-EI CORPORATION, with permission from SAN-EI CORPORATION.

Fig. 38

Reprinted from Cost-affordable Titanium (2004), pp. 185-192, Takamiya, H., Kondoh, M. and Saito, T., Ultra-high Pressure Warm Compaction for P/M Titanium Components, © 2004 TMS, with permission from John Wiley & Sons.

Fig. 43

Reprinted from Titanium '95: Science and Technology: Proc. 8th World Conf. Titanium (1995), pp. 2763-2770, Saito, T., Furuta, T. and Takamiya, H., Sintering Behavior and Thermal Stability of a TiB Particle Reinforced PM Beta-Titanium Matrix Composite, © 1995 The Institute of Materials, with permission from Taylor & Francis.

Tables 4-5

Reprinted from Recent Advances in Titanium Metal Matrix Composites: Proc. Symp. Held during Materials Week (1995), pp. 33-44, Saito, T., Furuta, T. and Yamaguchi, T., Development of Low Cost Titanium Matrix Composite, © 1995 TMS, with permission from The Minerals, Metals & Materials Society.

Takashi Saito

Research Fields:

- Physical Metallurgy
- Alloy Design
- Powder Metallurgy



Academic Degree: Dr.Eng.

Academic Societies:

- The Japan Institute of Metals and Materials
- The Iron and Steel Institute of Japan
- The Institute of Materials, Minerals and Mining
- Society of Automotive Engineers of Japan

Awards:

- Technical Development Award, The Japan Institute of Metals and Materials, 1994, 1995, 1996, 1998, 2004
- R&D 100 Award, 1996, 1998
- JSMS Award for Technical Developments, The Society of Materials Science, Japan, 1999
- Process Development Award, Japan Powder Metallurgy Association, 2000
- Technical Award, The Japan Titanium Society, 2000
- Dissertation Award, Gas Turbine Society of Japan, 2002
- Persons of Scientific and Technological Merits, Commendation by the Minister of Education, Culture, Sports, Science and Technology, Ministry of Education, Culture, Sports, Science and Technology, 2003